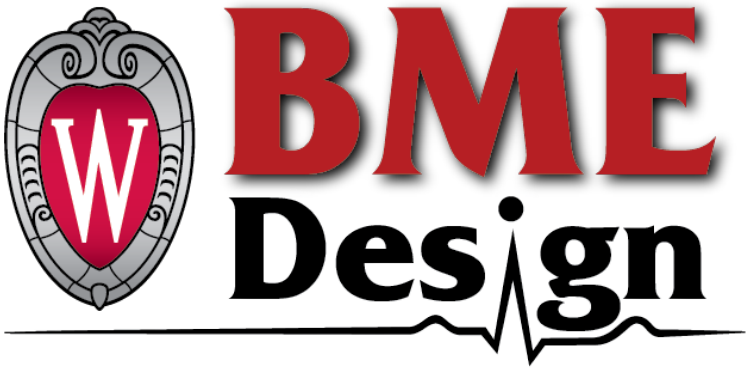

MRI Compatible Motion Platform

Final Report

BME 400

Team Members:
Maxwell Naslund - Team Leader

Kendra Besser - Communicator

Amber Schneider - BWIG

Jamie Flogel - BPAG

Caspar Uy - BSAC

Client:
Mr. Jiayi Tang - UW School of Medicine and Public Health Department of Medical Physics

Advisor:
Dr. James Trevathan - UW Institute for Translational Neuroengineering

December 13th, 2023

Abstract

Quantitative MRI (qMRI) can be used to quantify fat and mineral compositions of organs and is a minimally invasive diagnostic tool. MRI phantoms are widely used today as a means to test and calibrate the functionality of qMRI protocols. Static phantoms are often used for this purpose, but these do not give a good representation of the dynamic movements the body makes during imaging. To resolve this issue, motion platforms have been developed to replicate anatomical movement during phantom imaging; however, current devices on the market are costly and limiting in their use. A new proposed design will allow imaging of a wide range of phantoms, be fabricated from off-the-shelf components, and be cost effective such that it is applicable and accessible to other researchers. The final design consisted of a rack and pinion attached to a platform on linear rails. Sinusoidal motion was produced using an ultrasonic motor connected to a drive shaft and a gearbox. The gearbox translated the rotational motion from the motor and drive shaft into linear motion via the rack and pinion. Testing included optical tracking and motor RPM comparisons. Testing revealed experimental displacement was not consistent with the expected displacement. The RPM testing revealed a mismatch in input vs output RPM. Future work should be done primarily on the motor software, as well as minor mechanical improvements. Once this is done, more testing to validate MR compatibility as well as comparison with competing designs should be performed.

Table of Contents

Abstract **2**
Table of Contents **3**
I. Introduction **5**
A. Impact and Motivation 5
B. Existing Designs 5
C. Problem Statement 7
II. Background **7**
A. Physiology and Biology 7
B. Ultrasonic Motors and Preliminary Calculations 8
C. Design Specifications 9
D. Client Information 9
III. Preliminary Designs **10**
A. Lead Screw 10
B. Scotch Yoke 10
C. Rack and Pinion 11
IV. Preliminary Design Evaluation **12**
A. Design Matrix 12
Efficiency: 12
Accuracy: 13
Ease of Fabrication: 13
Cost: 13
Adjustability: 14
Safety: 14
Durability: 14
B. Proposed Final Design 15
V. Fabrication & Development Process **15**
A. Materials 15
B. Methods 15
Motor Assembly 15
Gearbox Assembly 15
C. Final Prototype 16
Microcontroller 17
Motor Assembly 17
Gearbox Assembly 18
Final Assembly 19
VI. Testing **19**
A. Motor Encoder Test 19

B. Motor RPM Test 20
C. Platform Sinusoidal Motion Test 20
VII. Results **20**
A. Motor Encoder Results 21
B. Motor RPM Results 21
C. Platform Sinusoidal Motion Results 22
VIII. Discussion **24**
IX. Conclusion **25**
X. References **27**
XI. Appendix **30**
A. Product Design Specifications 30
MRI Compatible Motion Platform - BME 400 30
B. Expense Table 35
Expenses 35
C. Fabrication Protocols 37
D. Testing Protocols 49
a. Platform Sinusoidal Motion Test 49
Description: **49**
Materials: **50**
Procedure: **50**
b. Motor RPM Test 50
Description: **50**
Materials: **51**
Procedure: **51**
c. Motor Encoder Test 51
Description: **51**
Materials: **52**
Procedure: **52**
E. Results Raw Data 52
F. Final Motor Code 53

I. Introduction

A. Impact and Motivation

Quantitative magnetic resonance imaging (qMRI) is a new and developing MR technique that measures specified characteristics of the tissues being imaged [1]. Healthcare professionals can utilize qMRIs to assist in many functions, such as detecting tissue characteristic changes over time, diagnosing and monitoring diseases, and determining drug efficiency [2] [3]. Specifically, qMRIs of livers can quantifiably characterize fat and iron compositions within the liver. This information can assist in the noninvasive detection and early diagnosis of diseases, such as steatosis [4]. Steatosis, also known as fatty liver disease, is an excessive accumulation of fat in a patient's liver. Steasosis affects about 25% of the world's population, typically targeting obese patients [5]. If left untreated steatosis can lead to further liver damage, cancer, or cirrhosis [5]. It is imperative to have accurate and effective qMRI techniques so that patients with steatosis can be treated immediately.

Current qMRI protocols require the patient to practice breath holds during the imaging to mitigate image artifacts [6]. Breath hold techniques can be very challenging for pediatric, elderly, severely ill, and sedated patients [7]. Developing a robust qMRI technique that can overcome respiratory motion will help support patients that can not perform breath holds. Aside from being not feasible for certain populations, the breath holding technique has short acquisition time to collect data. This sort acquisition time leads to decreased quality of imaging with a lower than ideal signal to noise ratio.

B. Existing Designs

Currently on the market there are some devices that are being used to produce motion within an MRI for testing of q-MRI protocols. In a study done by the Department of Radiology at University of Texas Southwestern Medical Center, researchers developed a one-dimensional MRI compatible motion platform. They used the platform in combination with an abdominal phantom to assess how movement during imaging affected the quality of images and the accuracy of quantitative metrics as shown below in Figure 1.

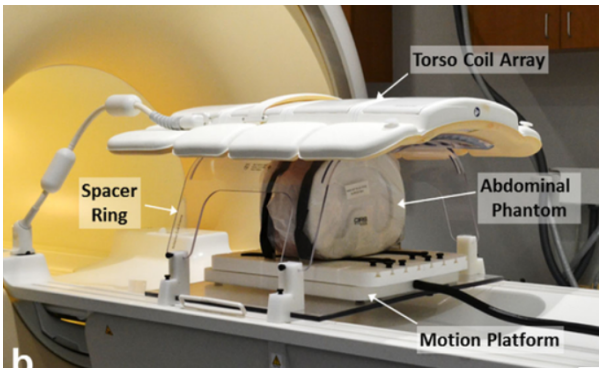

Figure 1. University of Texas Motion Platform [9]

This design consists of a motorized linear stage residing inside the MRI machine and driving electronics outside the MRI room. The motorized stage followed sinusoidal, harmonic, random, or user-defined trajectories. The device was used only for the study and is not on the market for outside use. Additionally this design was very costly, totaling around $19,000, and was specifically designed for an abdominal phantom [9].

Another competing design is the Vital Biomedical Technologies MRI Compatible Multi-Modality Motion Stage. This device is a programmable linear motion stage as shown below in Figure 2. This product is used in the bore of the MRI scanner and follows user-defined trajectories. The programmed trajectories are loaded onto the control system through a micro SD card.

Figure 2. Vital Biomedical Technologies MRI Compatible Motion Stage [11]

This product has a patent pending and there are a suite of other similar motion stages by this same company to address different anatomical motions [11]. Similar to the previous design this product is limited in phantom compatibility and cannot support the weight of a large phantom. Additionally, this product was also in the five figure range. Another drawback is that the motor is close to the phantom, which can create signal defects leading to inaccurate or imprecise q-MRI data.

The Quasar MRI Motion Phantom is an MR safe programmable phantom. In this device, the motion capable components are incorporated directly with the phantom as shown below in Figure 3.

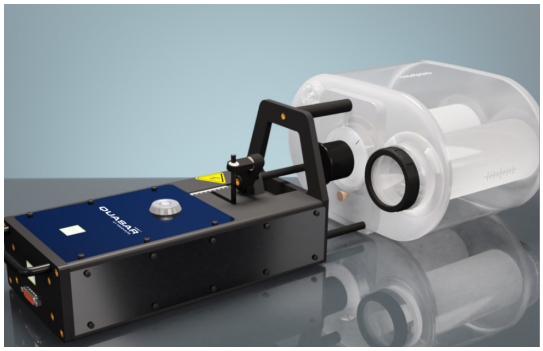

Figure 3. Quasar MRI Motion Phantom [12]

This design uses piezoelectric motors to create desired motions. It is intended to be used to test deep inspiration breath hold protocols. It is unclear how useful this product would be in

protocols that require normal respiratory movement rather than breath holding [12]. This was the most expensive of the three competing designs as the client received a quote near $50,000. In addition to the cost, this design limits what phantoms can be used as it can only hold specific cartridges provided by the company. This design also has motor components close to the phantom, which raises concerns about signal interference similar to the design by Vital Biomedical Technologies.

C. Problem Statement

Tissue phantoms used for the testing and calibration of quantitative magnetic resonance imaging (qMRI) are typically static replicas of the human body. However, these static models fall short in accurately capturing the continuous motion due to natural physiological processes, such as respiration and digestion. To address this limitation, a specialized MRI-compatible device capable of positioning a phantom and replicating physiological movements will be developed to enhance the accuracy of qMRI evaluations.

II. Background

A. Physiology and Biology

qMRIs map physiological characteristics by correlating the pixel intensity to a measurement of the specified physiological property. Examples of quantifiable characteristics that qMRIs can measure are nuclear magnetic resonance, relaxation times T1 and T2, diffusion and perfusion rates, fat and water fractions, iron fraction, elastic properties of tissue, temperature, chemical composition, and chemical exchange [13]. Figure 4, row B shows the qMRI map of liver fat fractions. This image compares a healthy liver (far left) to a steatotic liver (far right). Row C shows the percent fat in each liver with the steatotic liver being 75% composed of fat [4]. The figure shows how the qMRI map uses different color gradients to represent different fat concentrations across the liver sample.

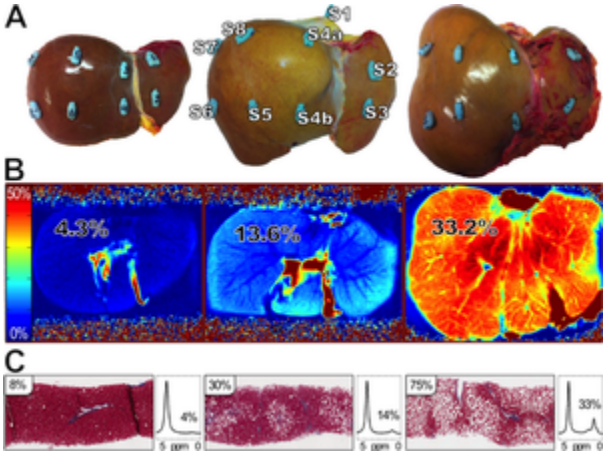

Figure 4. qMRI comparing health liver to steatotic liver [4]

Before testing tissue samples or scanning patients, qMRIs must be calibrated with precise software and phantoms with known values of the variable being tested [8]. Biological phantoms are also used to test the accuracy and precision of qMRIs and assist in research studies [10].

Developing a motion robust phantom for calibration and testing can enhance imaging results and eliminate the need for breath holds during scanning [14]. Movement during MRI scans can lead to motion artifacts which can cause inaccurate and imprecise data. Currently, the breath holding technique is used to reduce artifacts due to respiratory movement. This technique requires the patient to hold their breath for 10 to 30 seconds for multiple consecutive periods while being scanned [6]. Figure 5 shows the difference between an MRI image with breath holding and an MRI image without breath holding.

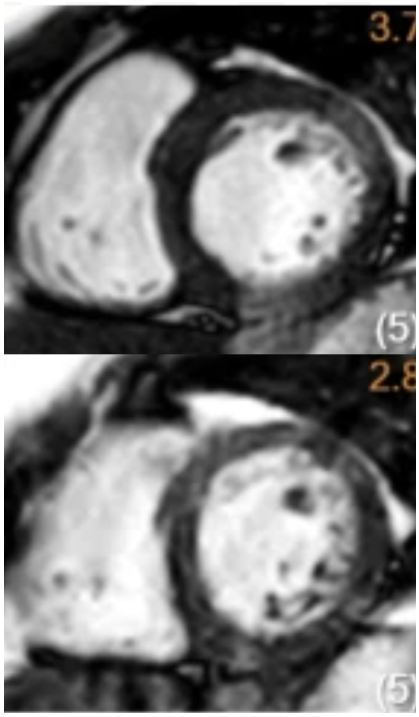

Figure 5. MRI with breath hold (top) and without (bottom) [7]

Developing qMRI techniques that can account for respiratory motion could allow for more accurate and comfortable diagnosis of diseases and conditions. Studies have been performed to track the movement of internal organs due to respirations using external signals [15]. Based on this data, liver movement due to respiration has been shown to be sinusoidal at a frequency of 8 cycles per minute and an amplitude of 3 cm [15].

B. Ultrasonic Motors and Preliminary Calculations

Figure 6 shows the nonmagnetic piezoelectric ultrasonic motor that will be used to create the motions of the phantom-holding platform. Although MRI safe, the ultrasonic motor can interfere with the radiofrequency field of the MRI magnet and produce image artifacts on the resulting image [16]. Therefore, the motor will be displaced the length of the MRI bed, 1.525 meters, from the MRI bore to reduce image artifacts.

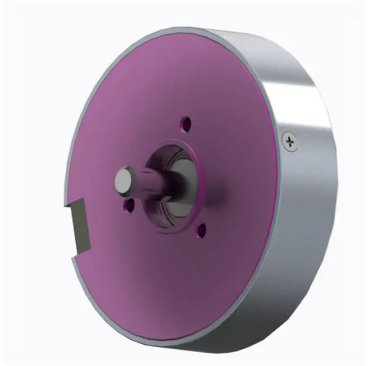

Figure 6. Nonmagnetic piezoelectric ultrasonic motor [17]

Using the data of a typical sinusoidal respiratory motion, the required motor torque was calculated. The torque was calculated by taking the second derivative of the position equation. The position equation is 3 cm × sin(2π×(8/60)×t). Taking the derivative with respect to time, the velocity is calculated to be 3 cm × (π×8/30) × cos(π×(8/30)×t). Taking the second derivative with respect to time, the acceleration is calculated to be 3 cm × $(\pi \times 8/30)^2$ × sin(π×(8/30)×t). From this equation, the maximum acceleration is determined to be 2.1 cm/s^2. The maximum acceleration, radius of the pinion, and estimated mass of 4 kg can be applied to the fundamental equation of torque, $\tau = rma$, to find the required maximum torque. The required torque is calculated by 21.64 cm × 4 kg × 2.1 cm/s^2 and found to be 1.82 ×10^{-3} N m. The motor specifications list a maximum torque of 1.2 N m; therefore, the motor is within the limits of the assembly [17].

C. Design Specifications

The most important specification of the design is that it is MR-compatible to assure it is safe to use in the MRI room as well as minimize signal interference to ensure accurate imaging results. The client has provided an initial budget of $1000 with more funds available if necessary. The client has emphasized making the design accessible and easy to replicate. Therefore, when possible, the motion platform should be designed using non-complex fabrication techniques and commercially available parts. This way other researchers and scientists, especially in places with limited funding, can analyze their own phantoms. In order to be compatible with liver phantoms, the platform should be able to support at least 4 kg and it must be larger than 25 cm by 35 cm [18]. In terms of motion capabilities, the product should be able to mimic physiologically realistic breathing patterns, which would be approximately 8 cycles per min with an amplitude of 3 cm [19]. The motion must be consistent for 10-15 minutes and within a standard deviation of 5% from the desired waveform [20]. For further specifications refer to Appendix A.

D. Client Information

Mr. Jiayi Tang is a PhD student at UW-Madison in the Department of Medical Physics as well as a research assistant in the Quantitative Imaging Methods Lab. His studies are focused on

the implementation, evaluation, and improvement of motion-robust qMRI sequences on liver phantoms.

III. Preliminary Designs

A. Lead Screw

The first design will utilize a lead screw to translate the rotational motion of the motor into the linear motion of the platform. As the motor rotates, the threads of the lead screw engage with a threaded attachment which either moves it forward or backward depending on the motor's direction. The lead screw in this design will be approximately 2 meters so the motor can be far from the platform to reduce image noise.

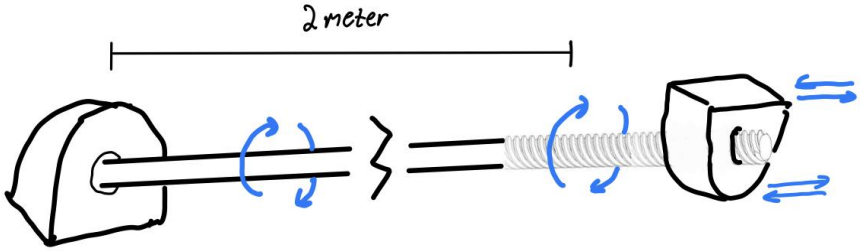

Figure 7. Lead Screw Design

Some benefits to this design include variable efficiency as you vary the helix angle of the screw. A higher helix angle allows for smoother motion, which reduces friction and improves the efficiency of power transfer, however, it also does require more torque [21]. Another benefit is that this mechanism works well for light loads, which is within the specifications outlined in the PDS (Appendix A). A drawback of this design is that the screw may wear out unevenly, causing a need for more frequent maintenance and replacement [21].

B. Scotch Yoke

The second design utilizes a scotch yoke to translate the rotational motion of the motor into the linear motion of the platform. As the motor rotates, the circular disc translates the motion into a back and forth movement, which is purely sinusoidal over time. The direction and distance of the linear motion are determined by the position of the pin along the radius of the disk. In order to get sufficient distance between the motor and the imaging platform, a set of bevel gears and a drive shaft will be used to translate the rotational motion 2 meters.

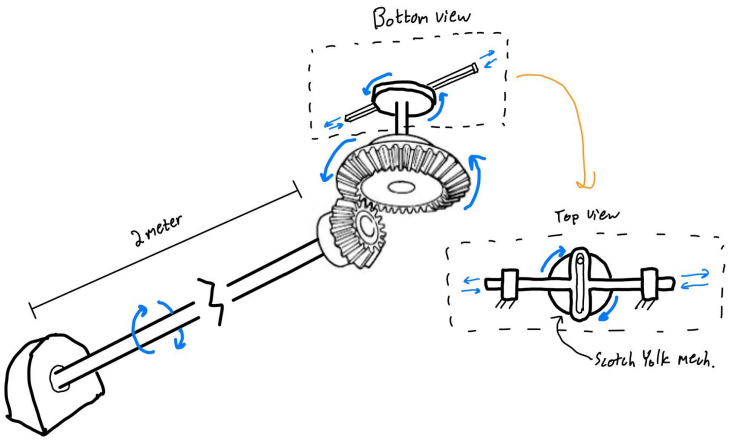

Figure 8. Scotch Yoke Design, including 2 bevel gears and a drive shaft

A benefit of this overall design is that it has variable torque depending on the angular position of the arm. The arm is longest at both ends of travel, which generates the most torque, and shortest at the midpoint, which generates the least torque [22]. This also has an inverse relationship with the speed of the linear motion. A drawback of this design is that the slot can wear out quickly due to friction and contact pressure [23].

C. Rack and Pinion

The third design utilizes a rack and pinion to translate the rotational motion of the motor into the linear motion of the platform. As the motor rotates, the gears of the fixed pinion engage with the teeth on the rack, causing it to move back and forth depending on the direction of the motor. Similar to the second design, a set of bevel gears and a drive shaft will be used to translate the rotational motion 2 meters.

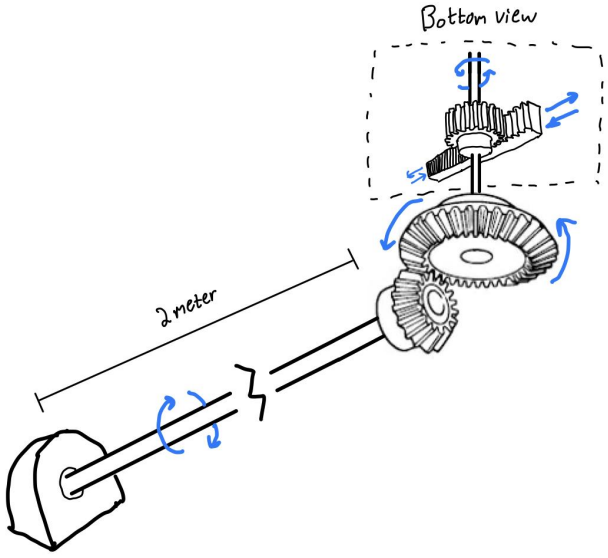

Figure 9. Rack and Pinion Design, including 2 bevel gears and a drive shaft

A benefit of this overall design is that it has efficiencies of up to 98.5%, allowing for smooth and accurate motion [24]. This mechanism is flexible to fit well with most applications by varying parameters such as pinion size, gear ratio, and damping levels [24]. A drawback of this design is it requires constant motor directional change, which leads to stress on the motor. Furthermore, any misalignment can damage parts and cause failures, so it is imperative to manufacture the components well [24].

IV. Preliminary Design Evaluation

A. Design Matrix

Table 1. Design Matrix of the three prototypes discussed above. Criteria are outlined on the left with the category winner highlighted in light green and the winning design highlighted in dark green.

Categories	Lead Screw		Scotch Yoke		Rack & Pinion	
Efficiency (25)	2/5	10	4/5	20	5/5	25
Accuracy (20)	5/5	20	3/5	12	4/5	16
Ease of Fabrication (15)	2/5	6	4/5	12	3/5	9
Cost (15)	4/5	12	3/5	9	2/5	6
Adjustability (10)	5/5	10	2/5	4	4/5	8
Safety (10)	4/5	8	2/5	4	4/5	8
Durability (5)	1/5	1	4/5	4	4/5	4
Total (100)		67		65		**76**

Once the product design specifications were fully developed, design criteria were generated to evaluate the effectiveness of the proposed designs. The designs were evaluated using the following criteria: Efficiency (25), Accuracy (20), Ease of Fabrication (15), Cost (15), Adjustability (10), Safety (10), and Durability (5).

Efficiency:

Currently the speed and shape of the waveforms produced by the design is greatly limited by the speed and torque produced by the piezoelectric motor. To accommodate this, the conversion of rotational motion to linear motion has to be done efficiently, hence its high weight in the design matrix. The Rack and Pinion design is the most efficient mechanism out of the three, which gives it the highest rating in this category. The Scotch Yoke design will inherently

have more friction in its conversion, which lowers its rating. The Lead Screw design by far has the most friction and is the least efficient in its conversion. This high friction causes the Lead Screw to have the lowest ranking of the three devices.

Accuracy:

As the design is hindered by the speed and torque of the piezoelectric motor, it is important to assure that the accuracy of the waveforms produced is not sacrificed at the cost of the efficiency of the device. The device has to be capable of producing a multitude of different waveforms that are easily differentiable from one another. The Lead Screw can be designed with a pitch that allows for high accuracy in the produced waveforms, this makes the Lead Screw the highest scoring design for accuracy. The Rack and Pinion can be designed with a high density of gear teeth, which will allow for increased precision and accuracy in the waveform produced. With increased gear teeth density, the Rack and Pinion becomes the second highest scoring design for accuracy. The waveform produced by the Scotch Yoke is limited by the location of the pin. This limitation of the waveform produced lowers the accuracy of the design overall and makes it the lowest ranking design in this criterion.

Ease of Fabrication:

The client highlighted the need for the device to be easy to fabricate. Many labs could benefit from having a device such as this, so its fabrication must be relatively easy to allow this design to be fabricated by others. Of the three preliminary designs, the Lead Screw design would likely be the hardest to fabricate. The Lead Screw of this design would likely have to be 3D-printed. For improved print quality, the screw would have to be printed vertically. The vertical height limit of 3D-printers would limit the overall length of the Lead Screw in the design. This process to develop the Lead Screw causes its design to be the lowest ranking of the three. The fabrication of the Scotch Yoke and Rack and Pinion designs would be relatively similar to each other. All components of both designs would be 3D-printed, so the Scotch Yoke design ranked as the best design in this criterion due to it requiring less material.

Cost:

Similar to ease of fabrication, the client wants this device to be easily accessible to labs. Therefore, the cost of the device should be as low as possible. All three designs utilize the same piezoelectric motor, and the rest of the components will be 3D-printed. This leads to the only cost differential between the three designs to be due to the amount of material each will consume to print. The Lead Screw design will consume the least amount of material to print, hence it was rated the best design in this category. The Scotch Yoke design would consume less material than the Rack and Pinion, leading to these designs being ranked 2nd and 3rd respectively.

Adjustability:

The device has to be capable of producing a multitude of different waveforms. It is important for this device to be easy to adjust to these different waveforms. This criterion measures how easy it is for the user to change what waveform is being output to the phantom bed of the design. The Lead Screw design rated the highest of the designs in this category due to its only limitation coming from the length of the screw. Any waveform with a magnitude within the length of the Lead Screw can be translated to the phantom bed. The Rack and Pinion design is similar in this respect, as it is also limited in its producible magnitude by the length of the rack. The Rack and Pinion design, however, is also limited by the required gearing ratio to transfer planes of rotation within the bevel gear box. This additional limitation makes this design the second highest scoring. The Scotch Yoke design is heavily limited by the radius at which the pin is located on the design. To change the sinusoidal waveform produced by this design, the pin on the Scotch Yoke would have to be physically moved by the user. This requirement makes the Scotch Yoke design undesirable when it comes to this criterion, and causes it to be ranked the lowest.

Safety:

This device must be able to fully function within an MRI and do so safely. Due to the high intensity magnetic fields being present within an MRI, it is vitally important that safety be considered when evaluating these designs. All three of these designs minimize the use of metal components to the same extent, so the only difference lies in how these devices might interact with the user. The Lead Screw and Rack and Pinion design both have minimal moving components and present the lowest pinch risk for the user when handling. Given this, the Lead Screw and Rack and Pinion design tied for best design for safety. The Scotch Yoke design has more moving components than the other two, leading to its lower ranking.

Durability:

This device is meant to be easy to fabricate and cost efficient. These two criteria tend to have an inverse relationship with durability, so it's important to consider this as a criterion as well. Durability, however, is not as vital of an aspect to this design as the others, so it has a lower weight. The Rack and Pinion design and the Scotch Yoke design both reduce friction to a great extent without the need of lubrication. This leads to these two designs being tied for the best in durability. The Lead Screw design inherently has a lot of friction in its mechanism, and would likely require periodic lubrication to prevent wear. Due to the high friction within the system, the Lead Screw design ranked the lowest for durability.

B. Proposed Final Design

Based on the design criteria above, the Rack and Pinion design emerged as the best overall design. This design ranked the best in efficiency and tied for best in safety and durability. It ranked second in accuracy, ease of fabrication, and adjustability, but last in cost. With all the benefits this design presents, it will be used moving forward.

V. Fabrication & Development Process

A. Materials

The prototype contains many 3D-printed parts, which were printed with PLA plastic to be MRI safe. For appropriate function and longer shelf life, all components will be non-conductive and non-metallic/magnetic. The platform will be made from a 1/4 acrylic sheet as 3D printing is not a viable option for such a large surface. The driveshaft responsible for separating the motor from the gearbox will be made of PVC to translate rotational motion across a long distance. The linear slides responsible for creating frictionless linear motion will be made of carbon fiber as they are non-metallic and off-the-shelf. The motor stand will be made of PLA as well as a copper sheet to hold the motor at the proper height and dissipate heat. For a full list of materials and their cost, see Appendix B.

B. Methods

The fabrication of the prototype can be broken down into 2 sections: motor assembly and gearbox assembly. A summary of the fabrication is described in this section. A full fabrication protocol can be found in Appendix C.

Motor Assembly

The motor assembly utilizes a WLG-75-R piezoelectric motor to generate rotational motion. This motor is controlled by a WLG-75-R-AMAG and Nucleo Board which is held outside of the MRI room, and connected via a long wire that spans the room. The motor is connected to a copper sheet to allow for heat dissipation. The copper sheet was machined in the TEAM Lab and is held upright at the proper height by a PLA base which was 3D-printed in the Makerspace. The motor is connected to a 5’ long, 3/4” nominal diameter PVC pipe driveshaft via an adaptor which was lathed out of 1” aluminum stock in the TEAM Lab. The motor assembly is then connected to the gearbox assembly via the driveshaft. See Figure 11 for motor part assembly.

Gearbox Assembly

The gearbox assembly converts the rotational motion provided by the motor into linear motion via a rack and pinion design. The driveshaft connects to the gearbox assembly via a machined adapter piece. This adaptor crosses into the gearbox through a glass ball bearing to

reduce rotational friction. The adapter then connects to a bevel gear to translate rotational motion to a perpendicular bevel gear within the gearbox. This perpendicular bevel gear is connected to a crosspin that extends through two sides of the gearbox, 180 degrees apart. The crosspin crosses through both sides of the gearbox through two glass ball bearings to further reduce friction. On both sides of the crosspin, pinion gears are attached. These pinion gears then interact with racks attached on top of the phantom bed. Linear slides are attached to the bottom of the phantom bed which can slide back and forth on linear rails. The linear rails are attached to the gearbox via gearbox extension pieces to accommodate the length of the rails. When rotational motion is passed to the gearbox assembly, the rack and pinion mechanism will cause the phantom bed to oscillate back and forth on top of the linear rails. The gearbox is only meant to shift rotational motion from the motor to a favorable plane, as such, the gearing ratio within the system is 1:1. To insure MR compatibility, the gearbox, gearbox extensions, bevel gears, and rack and pinion design were 3D printed in the Makerspace from PLA plastic. The driveshaft to gearbox adapter and crosspin were machined in the TEAM Lab from 1” HDPE cylindrical stock. The phantom bed was machined from acrylic in the TEAM Lab, while the linear rails and slides are made from carbon fiber and were provided by the client. See Figure 14 for gearbox part assembly.

C. Final Prototype

The final prototype consists of two sub-assemblies connected together via a 5’ driveshaft. One side of the driveshaft is the motor assembly which would sit on the end of the MRI bed. This motor assembly consists of a WLG-75-R piezoelectric motor held in place by a copper sheet. This copper sheet is screwed directly to the face of the motor, and provides a means to cool the motor. The motor is wired to a microcontroller that sits outside of the MRI room. This microcontroller is where sinusoidal waves are input to in turn control the motor. Rotational motion from the motor is transmitted down the driveshaft to the gearbox assembly which would sit within the MRI bore. The gearbox assembly converts rotational motion to linear motion via a rack and pinion. The translated linear motion will oscillate a phantom bed on the linear slides and rails according to the input sinusoidal wave.

Microcontroller

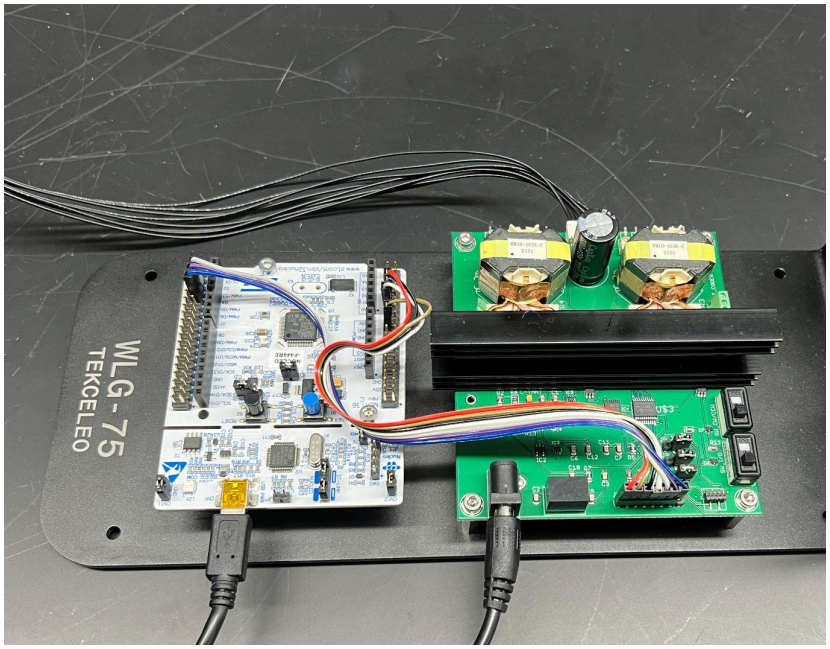

Figure 10. Final Prototype Microcontroller

Motor Assembly

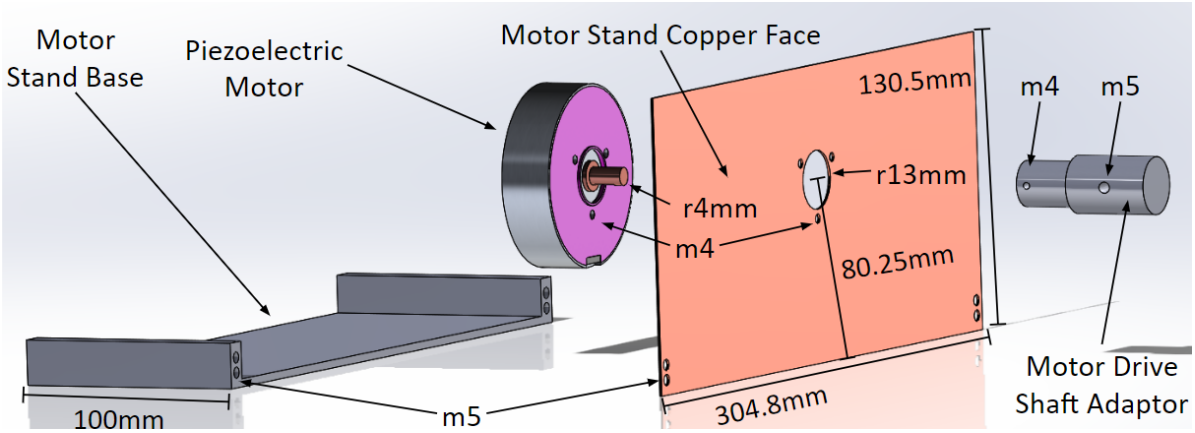

Figure 11. Motor Assembly SOLIDWORKS

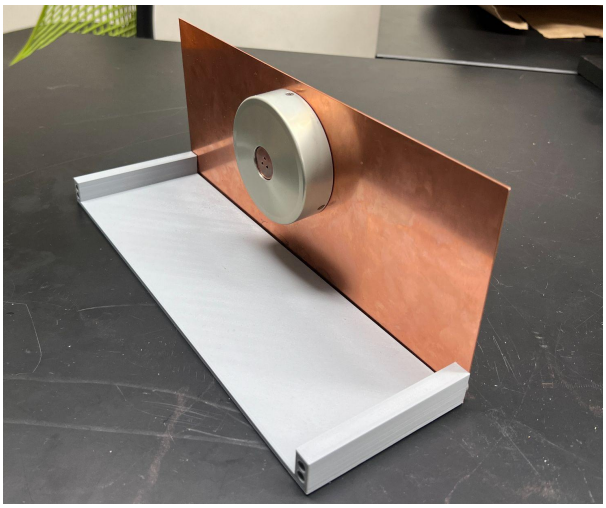

Figure 12. Motor Assembly Back

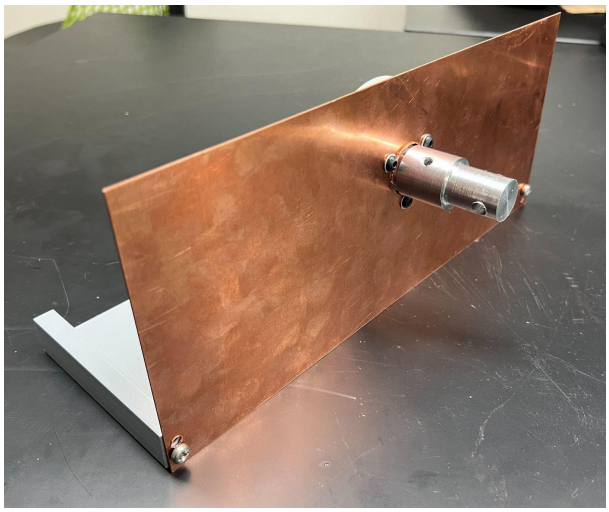

Figure 13. Motor Assembly Front

Gearbox Assembly

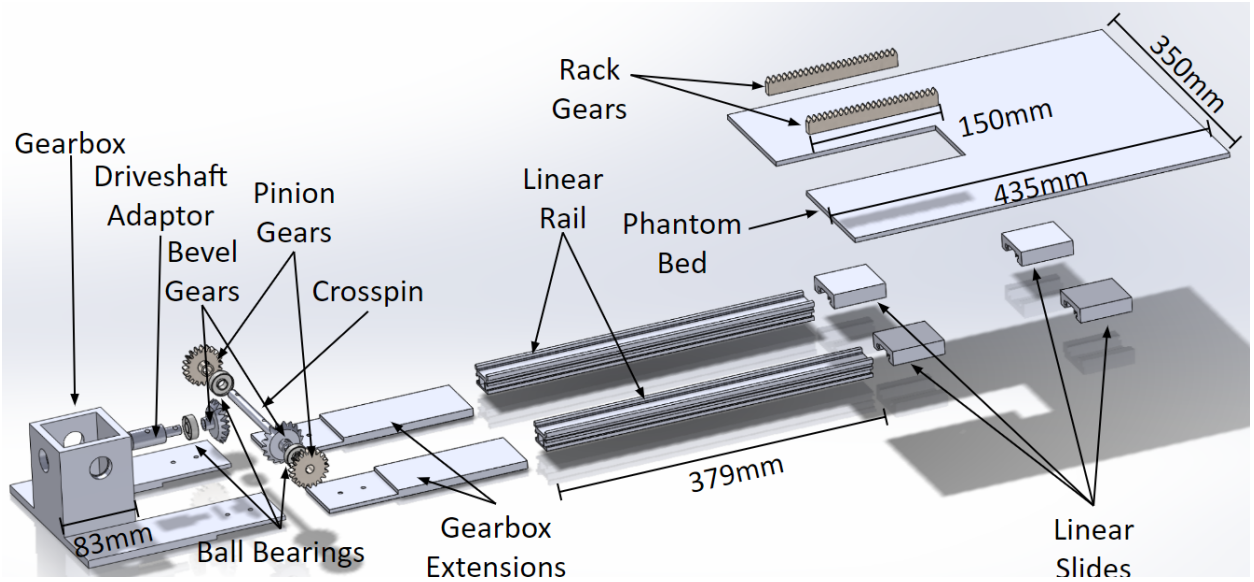

Figure 14. Gearbox Assembly SOLIDWORKS

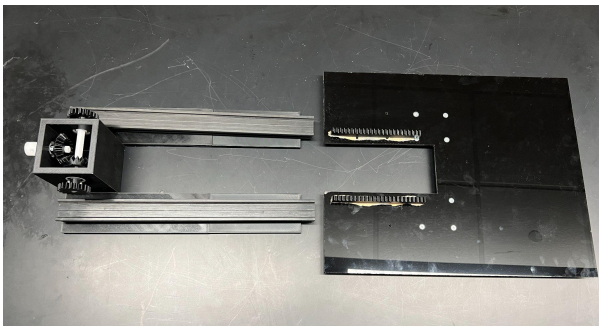

Figure 15. Gearbox Assembly Platform Removed

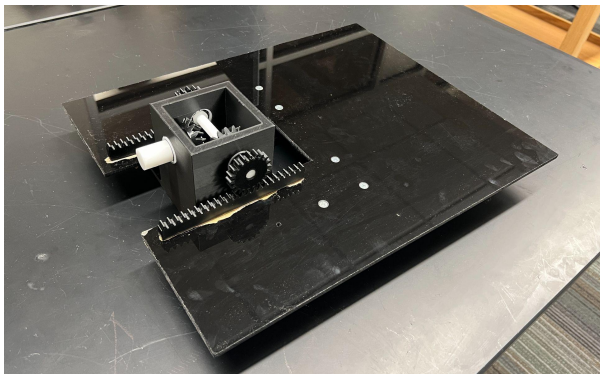

Figure 16. Gearbox Assembly Assembled

Final Assembly

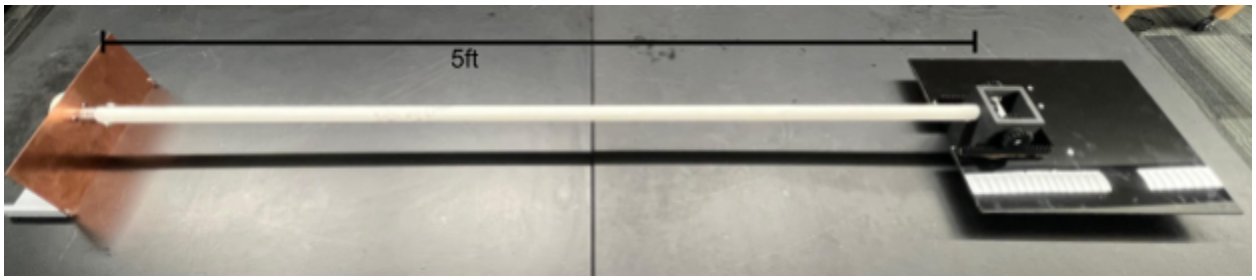

Figure 17. Final Assembly

VI. Testing

This semester, 3 tests were performed: motor encoder test, motor RPM test, and platform sinusoidal motion test.

A. Motor Encoder Test

This test is performed to determine if the number of revolutions counted by the motor encoder is accurate. It will reveal if there is any error associated with the built in encoder. This is important to determine its accuracy before relying on encoder values for motor control in the overall device. Additionally, it is important to validate the capabilities of the motor since it is MR compatible, which is a requirement of the PDS. For a full testing protocol refer to Appendix D. This test is performed on the motor only, disconnected from the prototype. To perform this test, place a thin flag on the motor shaft to mark initial position. Run “revolutionsCounter()” on Mbed by pressing 4. This program will rotate the motor at 60 RPM until the encoder counts 60 revolutions. During the test, visually count the number of rotations. Make note if the motor's final position is different from its starting position. The motor is expected to stop after 60 full

revolutions in the same position as it started. If the motor spins more or less than 60 revolutions during the test, then there is some error associated with the encoder values that needs to be addressed.

B. Motor RPM Test

This test is performed to determine if the rotations per minute of the motor is accurate. At programmed speeds the prototype will be assessed on how accurate the physical speed is compared to the expected speed. It will reveal if there is any error associated with the code to convert RPM to voltage to control the motor speed. This is important to determine the accuracy of the speed since the prototype's sinusoidal motion is dependent on this conversion. For a full testing protocol refer to Appendix D. This test is performed on the motor only, disconnected from the prototype. To perform this test, place a thin flag on the motor shaft to mark initial position. Begin recording a video in full view of the motor from above. Run "motorRPMTest()" on Mbed by pressing 5. This program will rotate the motor at a predetermined RPM (20, 40, or 60) until the encoder counts 1 revolution. Once complete, stop the recording. Measure the time it took to spin 1 revolution. The equation of the experimental RPM is 60/experiment_time. If the motor spins more or less than the expected RPM during the test, then there is some error associated with the RPM to voltage conversion that needs to be addressed.

C. Platform Sinusoidal Motion Test

This test is performed to determine if the platform is moving at the expected displacement of the sine wave. Trials will be conducted at different weights, but the motor velocity will be constant throughout trials. The prototype will be assessed on how accurate the displacement is over the course of the test in comparison to expected displacement. The expected displacement is calculated by taking the integral of the motor velocity with respect to time. Motor Velocity = $A \times \sin(2\pi \times f \times t)$, with A=10 RPM and f = 8/60 cycles per second, as determined by the PDS; therefore, Expected Displacement = $A/(2\pi \times f \times t) \times \cos(2\pi \times f \times t)$. This is important to determine if the accuracy of the sinusoidal motion is within 5% deviation, as specified in the PDS. For a full testing protocol refer to Appendix D. This test is performed on the entire prototype assembly. To perform this test, place a bright marker on the platform to mark the initial position. Begin recording a video in full view of the platform from above. Run "sinusoidalSpeedVariation()" on Mbed by pressing 2. This program will set the velocity of the motor to a sine wave that varies over time for 60 seconds. Once complete, stop the recording. Measure the displacement throughout the entire time the motor is moving. Identifying key aspects of the wave and comparing them to the expected wave will determine if the sinusoidal motion is within specifications, or if its accuracy needs to be improved.

VII. Results

Results of the tests described above are discussed in the following section. Raw testing data can be found in Appendix E.

A. Motor Encoder Results

The table below summarizes the data of the motor encoder test over 5 trials.

Table 2. Data of the motor encoder test.

Trial Number	Code Count	Visual Count
1	60	60
2	60	60
3	60	60
4	60	60
5	60	60

In all trials, the code count (expected) was equal to the visual count (theoretical). The difference between rotation counts was 0. There was no observable difference between the starting position and the ending position for any trial.

B. Motor RPM Results

Three RPM speeds were evaluated in the motor RPM testing. The results for the motor RPM test at 20 RPM is shown in the table below.

Table 3. Motor testing results at an expected speed of 20 RPM.

Trial Number	Expected RPM	Actual RPM
1	20	16.90
2	20	11.83
3	20	15.87
4	20	16.17
5	20	17.39

The average speed calculated is 15.63 RPM with a standard deviation of 2.21 RPM. The percent error is 21.83%. In all 5 trials, the experimental RPM was less than the expected RPM.

The results for the motor RPM test at 40 RPM is shown in the table below.

Table 4. Motor testing results at an expected speed of 40 RPM.

Trial Number	Expected RPM	Actual RPM
6	40	25.00
7	40	26.32
8	40	26.32
9	40	27.52
10	40	28.17

The average speed calculated is 26.66 RPM with a standard deviation of 1.23 RPM. The percent error is 33.34%. In all 5 trials, the experimental RPM was less than the expected RPM.

The results for the motor RPM test at 60 RPM is shown in the table below.

Table 5. Motor testing results at an expected speed of 60 RPM.

Trial Number	Expected RPM	Actual RPM
11	60	65.22
12	60	65.22
13	60	41.38
14	60	35.50
15	60	46.15

The average speed calculated is 50.69 RPM with a standard deviation of 13.8 RPM. The percent error is 15.51%. In 2 trials, the experimental RPM was greater than the expected RPM, while in the other 3 trials the experimental RPM was less than the expected RPM.

C. Platform Sinusoidal Motion Results

The sinusoidal motion test was performed with 0 kg of added weight and 4 kg of added weight. Plots of displacement over time were created for each trial. The expected displacement curve can be seen in orange, while the experimental displacement curve can be seen in blue.

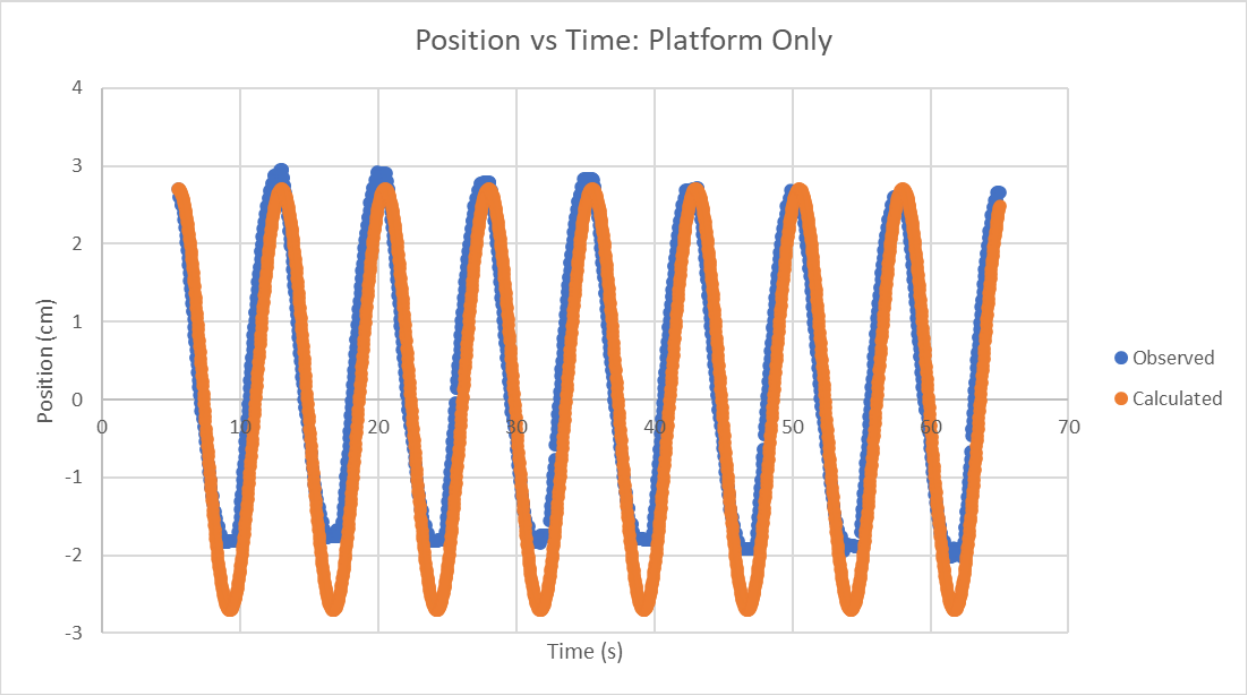

Figure 18. Position vs. Time graph with weight of the platform only.

The time between peaks was measured to be 7.50 ± 0.4 s with a 3.87% error. The expected value is 7.50 seconds, as determined by the set frequency of 8/60 cycles/s. The peak to peak amplitude was measured to be 4.619 ± 0.07 cm with a 14.63% error. The expected value is 5.41 cm, which is double the input of 10 RPM, which is equal to 2.705 cm/s. In this trial, the time between peaks is within the 5% tolerance set by the PDS, but the peak to peak amplitude is not.

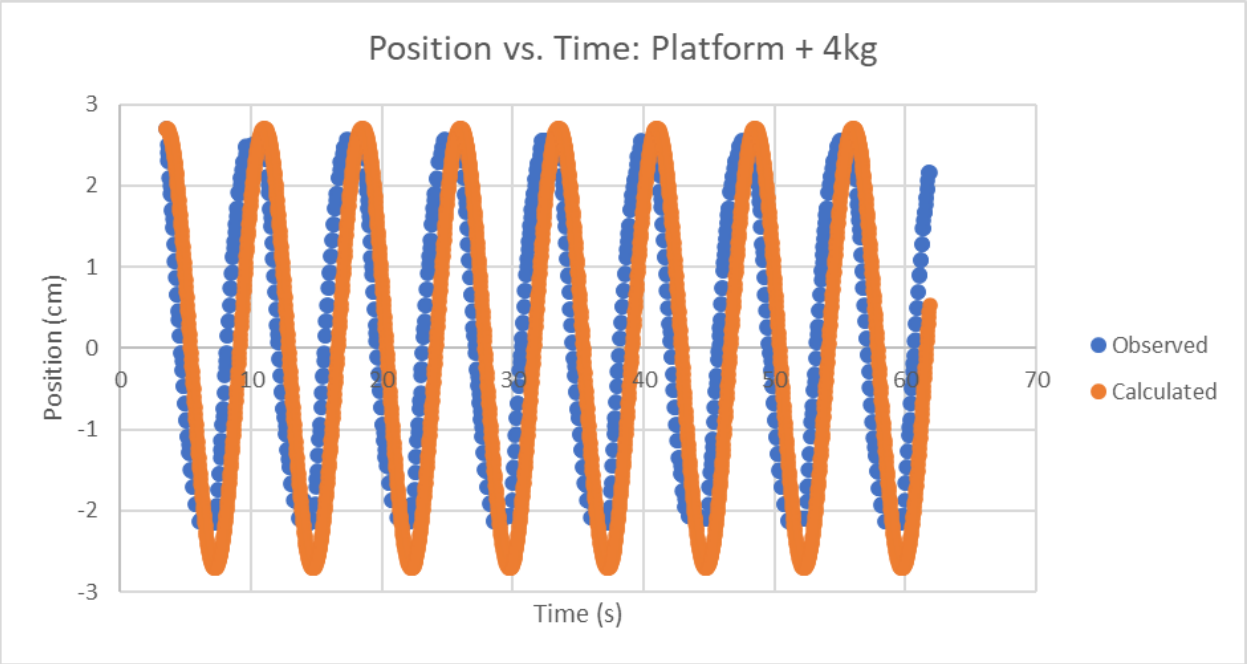

Figure 19. Position vs. Time graph with weight of the platform plus 4 kg.

The time between peaks was measured to be 7.50 ± 0.7 seconds with a 7.30% error. The expected value is 7.50 seconds, as determined by the set frequency of 8/60 cycles/s. The peak to peak amplitude was measured to be 4.685 ± 0.05 cm with a 13.39% error. The expected value is 5.41 cm, which is double the input of 10 RPM, which is equal to 2.705 cm/s. In this trial, the time between peaks and the peak to peak amplitude is not within the 5% tolerance set by the PDS.

VIII. Discussion

As this device is developed and ultimately used in the field, it is important to discuss ethical considerations. During development, it is important to maintain transparency with the client and research group who is funding the project. This includes sharing accurate information about project progress, setbacks, and limitations. This will establish clear accountability for the development and use of the technology. An additional consideration during development is that the final prototype is accessible and affordable. The prototype is meant to be affordable and accessible to a wide range of researchers, especially those who cannot afford current solutions. This goes hand in hand with the focus of this device to be open access. This helps promote advancement in medical research without barriers of intellectual property protection. Finally, safety and reliability should be prioritized to avoid harm to users of the technology. This can be ensured through future testing and validation of the device. It is important to continuously monitor and improve the technology to address any emerging ethical concerns or issues.

Three tests were performed this semester on different aspects of the prototype. The motor encoder test results were completely accurate, which supports the reliability of the motors built in encoder for future code development. At all speeds of the motor RPM tests, the observed

speed was slower than the expected speed. This test showed the RPM percent error to be 15% or greater. At higher speeds, the standard deviation was greater. As a result, the motor should be recalibrated in the RPM to voltage equation to improve the overall accuracy. The sinusoidal motion tests showed that the observed displacement wave led the calculated displacement wave in both trials. The displacement graphs for both trials exhibited sinusoidal motion similar to what was expected. When looking at the expected end point of the experiment, there was variation between the observed and calculated final positions. With increased weight, this difference was more prominent. The time between peaks was on average the most accurate, but at the desired 4 kg weight it did not meet the 5% specification outlined in the PDS. Both trials of peak to peak amplitude were outside of the PDS accuracy specification. In future improvements of the prototype, a closed loop feedback loop using the motor encoder will address the discrepancies between expected and actual displacement throughout the testing cycle.

There are many possible sources of error that could have impacted the test results described above. Further investigation into the mechanical and dynamic properties of the platform, particularly under varying loads, is necessary to identify and address the factors contributing to the observed deviations. Friction between sliders and play between gears can be improved to create more precise movement. The Kinovea tracking software used in many of the tests is limited in the precision it can provide for data collection. Given the metallic screws used in the proof of concept, rendering it non-MR compatible, transitioning to non-magnetic screws is essential for future MR environment testing. These enhancements will contribute to the future development of this device.

IX. Conclusion

The client for this project is Mr. Jiayi Tang, a PhD student at UW-Madison in the Department of Medical Physics. He has proposed that developing a MR-compatible motion platform that is more cost effective and accessible would allow researchers to more accurately evaluate qMRI protocols. Currently, products that are designed for this function are limited to specific phantoms and are extremely expensive. This technology would improve diagnostic capabilities for patients currently unable to perform current image artifact mitigation procedures, such as deep inspiration breath hold protocols.

While there are different modalities for producing linear motion, a design that features a rack and pinion allows for precise control, high power conversion efficiency, and high durability. The final design featured a 3D printed gearbox which converted rotational motion from an ultrasonic motor to the phantom bed. The rack was screwed into an acrylic platform which sat on linear slides to reduce friction. The motor was programmed to produce a sine wave to mimic anatomical breathing.

Testing included optical tracking of the platform unloaded vs loaded as well as motor RPM testing. Movement data was tracked and analyzed using Kinovea. The experimental sine wave was compared to the one imputed into the motor. A comparison of peak to peak times as well as amplitudes proved that experimental motion did not properly track with the input sine

wave. RPM testing revealed that the input motor RPM was significantly higher than what was being output by the motor. This was likely a key factor in the movement discrepancy that was found.

Before testing for MRI compatibility and accuracy in phantom imaging, modifications to the motor code should be made. Additionally, more work can be done to reduce play between gears and reduce friction on the sliders. Overall with modifications, this design has the potential to be an important research tool for the validation and testing of qMRI protocols.

X. References

[1] “Broadening the Use of Quantitative MRI, a New Approach to Diagnostics,” Stanford HAI. Accessed: Oct. 09, 2023. [Online]. Available: https://hai.stanford.edu/news/broadening-use-quantitative-mri-new-approach-diagnostics

[2] A. Seiler et al., “Multiparametric Quantitative MRI in Neurological Diseases,” Front. Neurol., vol. 12, 2021, Accessed: Oct. 09, 2023. [Online]. Available: https://www.frontiersin.org/articles/10.3389/fneur.2021.640239

[3] K. E. Keenan et al., “Recommendations Towards Standards for Quantitative MRI (qMRI) and Outstanding Needs,” J. Magn. Reson. Imaging JMRI, vol. 49, no. 7, pp. e26–e39, Jun. 2019, doi: 10.1002/jmri.26598.

[4] P. Bannas et al., “Quantitative magnetic resonance imaging of hepatic steatosis: Validation in ex vivo human livers,” Hepatology, vol. 62, no. 5, pp. 1444–1455, Nov. 2015, doi: 10.1002/hep.28012.

[5] “Nonalcoholic fatty liver disease - Symptoms and causes,” Mayo Clinic. Accessed: Oct. 09, 2023. [Online]. Available: https://www.mayoclinic.org/diseases-conditions/nonalcoholic-fatty-liver-disease/symptoms-causes/syc-20354567

[6] D. A. Feinberg, N. M. Rofsky, and G. Johnson, “Multiple breath-hold averaging (mba) method for increased snr in abdominal mri,” Magn. Reson. Med., vol. 34, no. 6, pp. 905–909, 1995, doi: 10.1002/mrm.1910340617.

[7] M. Kocaoglu, A. S. Pednekar, H. Wang, T. Alsaied, M. D. Taylor, and M. S. Rattan, “Breath-hold and free-breathing quantitative assessment of biventricular volume and function using compressed SENSE: a clinical validation in children and young adults,” J. Cardiovasc. Magn. Reson., vol. 22, no. 1, p. 54, Jul. 2020, doi: 10.1186/s12968-020-00642-y.

[8] “About,” CaliberMRI. Accessed: Dec. 11, 2023. [Online]. Available: https://qmri.com/about/

[9] W. T. Reichert, “A Simple Multi-Parametric Quantitative MRI Phantom”.

[10] J. Nofiele et al., “An MRI-Compatible Platform for One-Dimensional Motion Management Studies in MRI,” Magnetic resonance in medicine, vol. 76, no. 2, p. 702, Aug. 2016, doi: 10.1002/mrm.25903.

[11] “Motion Stages Compatible with CT, MRI, PET, SPECT & Ultrasound.” https://www.simutec.com/Products/motionstages.html (accessed Sep. 20, 2023).

[12] “QUASARTM MRI4D Motion Phantom,” Modus Medical Devices. https://modusqa.com/products/quasar-mri4d-motion-phantom/ (accessed Sep. 20, 2023).

[13] V. Gulani and N. Seiberlich, “Quantitative MRI: Rationale and Challenges,” in Advances in Magnetic Resonance Technology and Applications, vol. 1, N. Seiberlich, V. Gulani, F. Calamante, A. Campbell-Washburn, M. Doneva, H. H. Hu, and S. Sourbron, Eds., in Quantitative Magnetic Resonance Imaging, vol. 1. , Academic Press, 2020, pp. xxxvii–li. doi: 10.1016/B978-0-12-817057-1.00001-9.

[14] C. Arboleda et al., “Total liver fat quantification using three-dimensional respiratory self-navigated MRI sequence,” Magnetic Resonance in Medicine, vol. 76, no. 5, pp. 1400–1409, 2016, doi: 10.1002/mrm.26028.

[15] S. Fahmi, F. F. J. Simonis, and M. Abayazid, “Respiratory motion estimation of the liver with abdominal motion as a surrogate,” Int J Med Robot, vol. 14, no. 6, p. e1940, Dec. 2018, doi: 10.1002/rcs.1940.

[16] P. Shokrollahi, J. M. Drake, and A. A. Goldenberg, “A study on observed ultrasonic motor-induced magnetic resonance imaging (MRI) artifacts,” Biomed. J., vol. 42, no. 2, pp. 116–123, Apr. 2019, doi: 10.1016/j.bj.2018.12.007.

[17] “WLG-75-R - Rotary piezoelectric motor by TEKCELEO | DirectIndustry.” Accessed: Oct. 04, 2023. [Online]. Available: https://www.directindustry.com/prod/tekceleo/product-191564-2441488.html

[18] “Liver Phantom — The Phantom Laboratory.” https://www.phantomlab.com/liver-phantom (accessed Sep. 22, 2023).

[19] J. Nofiele et al., “An MRI-Compatible Platform for One-Dimensional Motion Management Studies in MRI,” Magnetic resonance in medicine, vol. 76, no. 2, p. 702, Aug. 2016, doi: 10.1002/mrm.25903.

[20] J. Tang, J. Rice, J. Gwertzman, S. Reeder, A. Roldán-Alzate, and D. Hernando, “Development of an MR-Compatible Motion Phantom to Evaluate Motion-Robust Quantitative MRI”, Accessed: Sep. 11, 2023. [Online]. Available: https://uwmadison.app.box.com/s/fp4knxj8nk4ww1j3frqtb91l75v0v2a0

[21] “Why lead screws best fit linear motion applications,” Thomson Linear, https://www.thomsonlinear.com/downloads/articles/Why_Lead_Screws_Best_Fit_Linear_Motion_Applications_taen.pdf (accessed Oct. 4, 2023).

[22] Rotork, “Fluid Power Actuators explained,” Rotork Fluid Systems, https://www.rotork.com/uploads/documents-versions/24733/1/pub010-024-00_0516.pdf (accessed Oct. 7, 2023).

[23] “Scotch Yoke Mechanism: Working, Advantages and Applications.,” Testbook. Accessed: Oct. 04, 2023. [Online]. Available: https://testbook.com/mechanical-engineering/scotch-yoke-mechanism-application

[24] M. Anselmo, “How do Rack-and-Pinion Drives Stack up Against Other Linear Motion Systems?,” Machine Design. Accessed: Oct. 04, 2023. [Online]. Available: https://www.machinedesign.com/mechanical-motion-systems/article/21831764/how-do-rackandpinion-drives-stack-up-against-other-linear-motion-systems

XI. Appendix

A. Product Design Specifications

MRI Compatible Motion Platform - BME 400

Product Design Specifications
September 22nd, 2023

Client:	Mr. Jiayi Tang
Advisor:	Dr. James Trevathan
Team:	Maxwell Naslund - Team Leader
	Kendra Besser - Communicator
	Amber Schneider - BWIG
	Jamie Flogel - BPAG
	Caspar Uy - BSAC

Function

MRI phantoms are often static models of the human body that are used to test and calibrate MRI's. Natural process' such as respiration and digestion create constant motion within the human body. Static phantoms used to calibrate MRI's do not properly represent this motion. This demonstrates a need for an MR compatible device that holds a phantom and is capable of simulating the movements found within the human body.

Client requirements:

- MR Compatible
- Moves back and forth
- Minimize the use of electronics inside the room
- Potentially incorporate materials currently available from the client
- Create a prototype with a budget of $1000
- Utilize commercially available parts
- Avoid complex fabrication methods

Design requirements:

1. Physical and Operational Characteristics

a. *Performance requirements*: The product will be a magnetic resonance compatible platform that provides a periodic waveform motion. The waveform motion will have a frequency of 8 cycles/min and amplitude of 3 cm to represent physiological breathing patterns. The motion will be consistent for 10-15 minutes and is allotted a standard deviation of 5% from the desired waveform. The product must withstand the size and weight of a phantom liver for testing purposes.

b. *Safety*: The device will be entirely made of MR compatible material and will pose no safety risk within the MR environment. The device's magnetically induced displacement and torque forces will be tested to assure these forces are below their gravitational equivalents. The device will also be evaluated for RF heating, eddy currents, gradient induced vibrations, and gradient induced extrinsic electrical potential risks, as also recommended by the FDA [1]. As this device will utilize electronics, it is classified as an active medical device and will follow FDA 21 CFR part 801 and ASTM F2503 labeling requirements.

c. *Accuracy and Reliability*: The device must be able to produce repeatable patterns of movements within 2mm. The components of the device must not decrease the signal to noise ratio of the calibration phantom being tested. The device must be able to reliably repeat MR scans with minimal decrease in image quality between scans.

d. *Life in Service*: The device must operate for up to 60 minutes at a time as that is the time an MRI may take to produce an image of a medium-sized area [2]. A non-magnetic motor should last 20,000 hours under normal operating conditions [3]. Overall the device should last as long as an MRI scanner, which is approximately 10 years [4].

e. *Shelf Life*: Based on the motor components it should be stored in -40 to 70 °C temperatures with humidity 0 to 80% non condensing [2].

f. *Operating Environment*: The device must be able to withstand upwards of 3 tesla for 1 hour [5]. The device must be able to withstand potential RF heating, eddy currents, gradient induced vibrations, and gradient induced extrinsic electrical potential risks associated with devices within strong magnetic fields [1].

g. *Ergonomics*: The platform should have a height that is comfortable and safe for people to interact with when placed in the MRI. No force should be applied by a person to the motor or any moving parts during operation. An emergency stop feature should be implemented to allow users to immediately stop the motion platform in case of any issues or safety concerns.

h. *Size*: The platform will be no smaller than 25cm x 35cm in order to hold a range of phantom liver samples [6]. The platform will be rectangular shaped.

i. *Weight*: In order for the user to install and uninstall the platform during each segment of testing, the weight should not exceed 10kg. The platform must be able to withstand 4kg [7].

j. *Materials*: The product will be composed of MRI compatible materials. Ferrous and magnetic metals will not be used; other metals, such as brass and aluminum, will be limited to minimize the possibility of induced currents. A nonmagnetic ultrasonic piezoelectric motor will be used to provide platform motion. Nonmetalic sliding rails and bearings will be used to guide the platform through the MRI machine.

k. *Aesthetics*, *Appearance, and Finish*: Color, shape, form, texture of finish should be specified where possible (get opinions from as many sources as possible).

2. Production Characteristics

a. *Quantity*: Produce one motion controlled platform.

b. *Target Product Cost*: The budget for this project is $1000 with many of the components already provided including some motors, rails, software, and hardware. Existing MRI compatible designs cost around $9700 excluding the cost of the phantom used [7].

3. Miscellaneous

a. *Standards and Specifications*: MRI systems and accessories must follow the multiple sets of standards designed by the organizations like the FDA involving forms of testing the functionality of the machine including any additional accessories. Accessory parts should allow appropriate function in testing MRI displacement force ASTM F2052, torque ASTM F2213, RF heating ASTM F2182, and image artifact ASTM F2119 [8].

b. *Customer*: Preferences on stability and levelness will assist users in creating more genuine images. Reducing additional noise from both the platform and machine would be beneficial to more optimal usage.

c. *Patient-related concerns*: The device would need to be appropriately cleaned and disinfected for each use as instructed with the associated manufacturer. Appropriate dimensions levelness of the platform will need to be monitored to help with specimen/subject safety. Additionally cleanliness of the machine is an important consideration as the device should not leak motor oil or other fluids on the MRI bed.

d. Competition:

- Vital Biomedical Technologies MRI Compatible Multi-Modality Motion Stage is a programmable linear motion stage. This product is used in the bore of the MRI scanner and follows user-defined trajectories. The programmed trajectories are loaded onto the control system through a micro SD card. This product has a patent pending and there are a suite of other similar motion stages by this same company to address different anatomical motions [9].
- For a study done by the Department of Radiology at University of Texas

Southwestern Medical Center researchers developed a one-dimensional MRI compatible motion platform. They used this in combination with an abdominal phantom to assess how movement during imaging affected the quality of images and the accuracy of quantitative metrics. This design consisted of a motorized linear stage residing inside the MRI machine and driving electronics outside the MRI room. The motorized stage followed sinusoidal, harmonic, random or user-defined trajectories. The device was used for the study and is not on the market for outside use [7].

- The Quasar MRI Motion Phantom is a completely MR safe programmable phantom. In this device the motion capable components are incorporated directly with the phantom. This design uses piezoelectric motors to create desired motions. It is intended to be used to test deep inspiration breath hold protocols. It is unclear how useful this product would be in protocols that require normal respiratory movement rather than breath holding [10].

References

[1] “Testing and labeling medical devices for safety in the magnetic ...,” U.S. FOOD & DRUG ADMINISTRATION, https://www.fda.gov/media/74201/download?attachment (accessed Sep. 22, 2023).

[2] “How it’s performed - MRI Scan,” NHS choices, https://www.nhs.uk/conditions/mri-scan/what-happens/#:~:text=A%20magnetic%20resonance%20imaging%20(MRI,number%20of%20images%20being%20taken. (accessed Sep. 20, 2023).

[3] “Hr4 nanomotion motor ,” NANOMOTION, https://www.nanomotion.com/product/hr4-nanomotion-motor/ (accessed Sep. 20, 2023).

[4] A. Sahu, H. Vikas, and N. Sharma, “Life cycle costing of MRI machine at a tertiary care teaching hospital,” The Indian journal of radiology & imaging, https://www.ncbi.nlm.nih.gov/pmc/articles/PMC7546299/ (accessed Sep. 20, 2023).

[5] K. Albus, “Small phantom testing: MRI (revised 3-6-23),” Accreditation Support, https://accreditationsupport.acr.org/support/solutions/articles/11000061036-small-phantom-testing-mri-revised-3-6-23- (accessed Sep. 21, 2023).

[6] “Liver Phantom — The Phantom Laboratory.” https://www.phantomlab.com/liver-phantom (accessed Sep. 22, 2023).

[7] J. Nofiele *et al.*, “An MRI-Compatible Platform for One-Dimensional Motion Management Studies in MRI,” *Magnetic resonance in medicine*, vol. 76, no. 2, p. 702, Aug. 2016, doi: 10.1002/mrm.25903.

[8] Center for Devices and Radiological Health. “MRI Information for Industry.” U.S. Food and Drug Administration, FDA, www.fda.gov/radiation-emitting-products/mri-magnetic-resonance-imaging/mri-information-industry. Accessed 20 Sept. 2023.

[9] “Motion Stages Compatible with CT, MRI, PET, SPECT & Ultrasound.” https://www.simutec.com/Products/motionstages.html (accessed Sep. 20, 2023).

[10] “QUASAR™ MRI4D Motion Phantom,” *Modus Medical Devices*. https://modusqa.com/products/quasar-mri4d-motion-phantom/ (accessed Sep. 20, 2023).

B. Expense Table

Expenses

Item	Description	Manufacturer	Part Number	Date	QTY	Cost Each	Total	Link
Component 1								
Ultimaker PLA (37.0 g)	3D printed gears to translate and facilitate motion	Ultimaker	RAL-9010	10/26/2023	1	$2.96	$2.96	N/A
Ultimaker PLA (325.0 g)	3D printed gears and gearbox	Ultimaker	RAL-9005	11/03/2023	1	$26.00	$26.00	N/A
Bamboo Labs PLA (127.34 g)	3D printed gearbox extension pieces	Bambu Lab	#000000	11/15/2023	1	$12.19	$12.19	N/A
Ultimaker PLA (118 g)	3D printed support for the driveshaft	Ultimaker	RAL-9005	11/17/2023	1	$9.44	$9.44	N/A
Ultimaker PLA (27 g)	3D printed racks	Ultimaker	RAL-9005	11/29/2023	1	$2.16	$2.16	N/A
Ultimaker PLA (126 g)	3D printed Motor Stand	Ultimaker	RAL-9005	12/01/2023	1	$10.08	$10.08	N/A

Component 2								
Linear Rails	400 mm linear rails	igus	CWS-06-30-400	11/13/2023	2	$167.69	$335.38	Link
Component 3								
Linear Slides	Slides to support platform on linear slides	igus	WWPL-06-30-06	11/13/2023	2	$18.25	$36.50	Link
Component 4								
Driveshaft	Connection piece between motor and gearbox	Grainger	H0400075PW1000	11/16/2023	1	$8.00	$8.00	Link
Component 5								
Platform	1/4 black acrylic sheet provided by Makerspace	MSC	MSC# 63391700 (similar example as no part number given by makerspace)	11/17/2023	1	$20.00	$20.00	N/A
Component 6								

Glass Ball Bearings	Glass ball bearings to allow for frictionless rotation	Grainger	MSN0459939	12/1/2023	5	$17.07	$85.35	N/A
Component 7 - unused features due to reprints/redesigns								
Ultimaker PLA	3D printed Gearbox	Ultimaker	RAL-9005	10/26/2023	1	$19.36	$19.36	N/A
Ultimaker PLA	Motor to driveshaft adapter piece	Ultimaker	RAL-9005	12/1/2023	1	$1.12	$1.12	N/A
Ultimaker PLA	Motor to driveshaft adapter piece reprint	Ultimaker	RAL-9005	12/4	1	$2.84	$2.84	N/A
Ultimaker PLA	Motor to driveshaft adapter piece reprint	Ultimaker	RAL-9005	12/5	1	$2.65	$2.65	N/A
TOTAL:	**$574.03**							

C. Fabrication Protocols

Motor Assembly

Copper Face

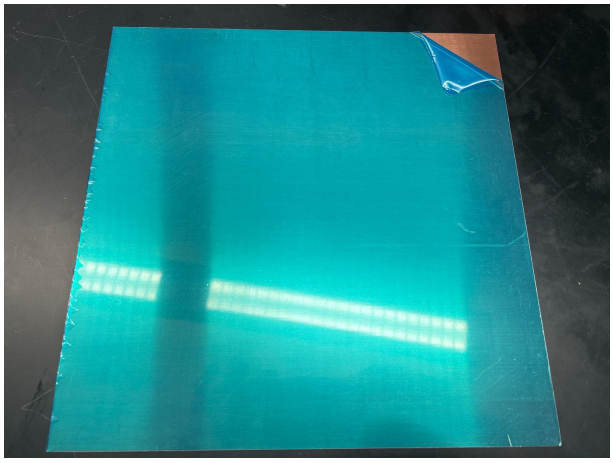

Figure 1: Uncut 1’ x 1’ copper sheet

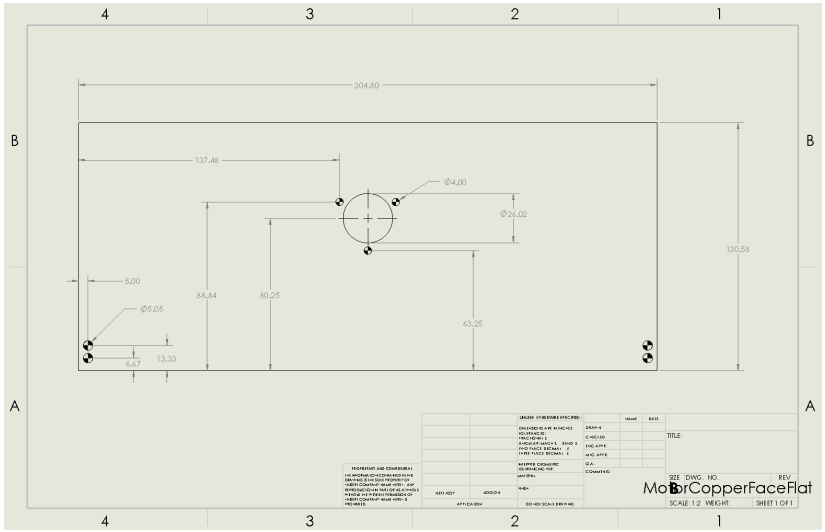

Figure 2: Copper face drawing

1. Starting from the 1’ x 1’ copper sheet illustrated in figure 1, on the metal shear in the. TEAM Lab, cut a piece to 130.58cm tall.
2. Drill a pilot hole in the cut copper sheet at 152.4mm in the x-dimension, and 88.84mm in the y-direction as illustrated in figure 2.
3. Using a 1” hole saw, drill a 1” hole centered at the previously drilled pilot hole.
4. Drill three 3mm holes 120 degrees apart around the previously drilled 1” hole as illustrated in figure 2.
5. Drill four 5mm holes at the locations illustrated in figure 2.

Motor Stand

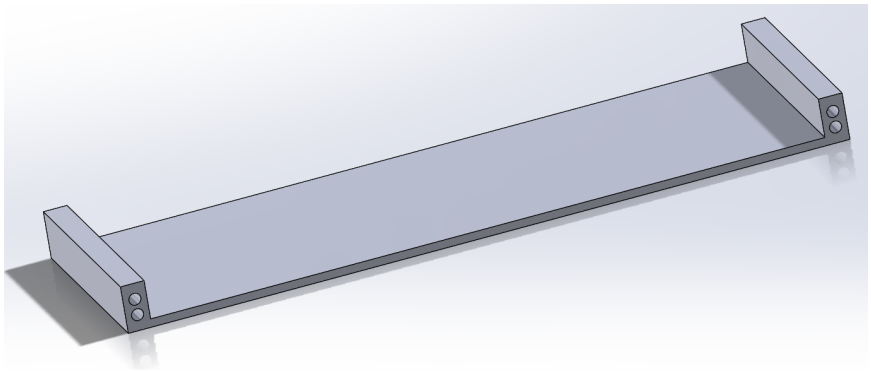

Figure 3: Motor stand SOLIDWORKS

1. 3D print attached motor stand .stl file at the Makerspace with 20% infill.

Motor to Driveshaft Adapter

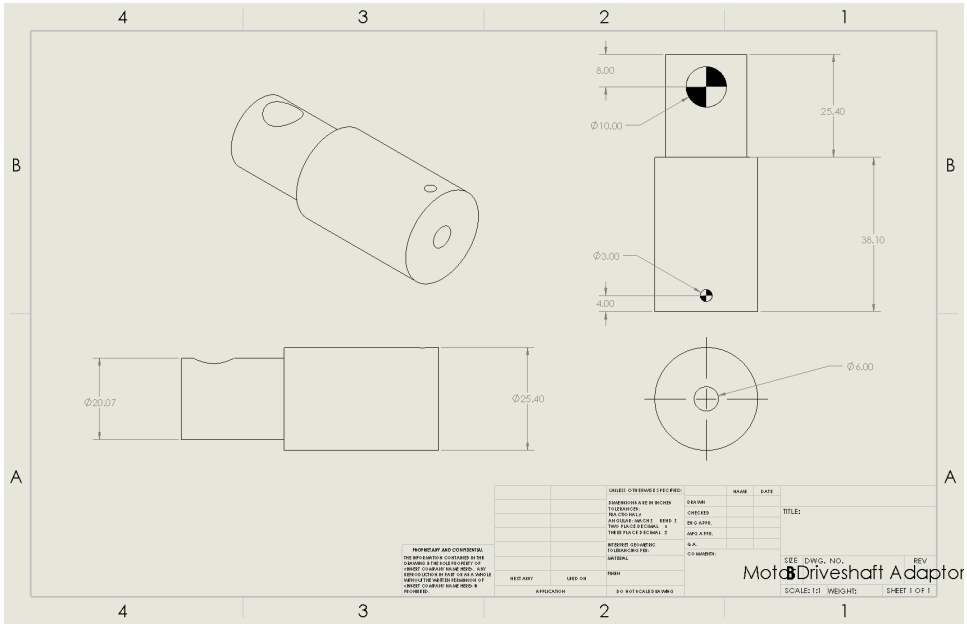

Figure 4: Driveshaft to Driveshaft Adapter drawing

1. Starting from 1” cylindrical aluminum stock, lathe one side down to a 20.07mm diameter 25.4mm in the TEAM Lab, as illustrated in figure 4.
2. Using a 6mm bit, drill a center hole 19mm deep on the side of the stock that is 25.4mm, as illustrated on figure 4.
3. Part the cylindrical aluminum stock off at 63.5mm, as illustrated in figure 4.
4. On the mill, drill a 3mm hole 4mm from the end of the 25.4mm end of the part. Drill down to the center hole drilled on the lathe, as illustrated on figure 4.
5. On the mill, drill a 10mm hole 8mm from the end of the 20.07mm end of the part. Drill all the way through the part, as illustrated on figure 4.

Full Motor Assembly

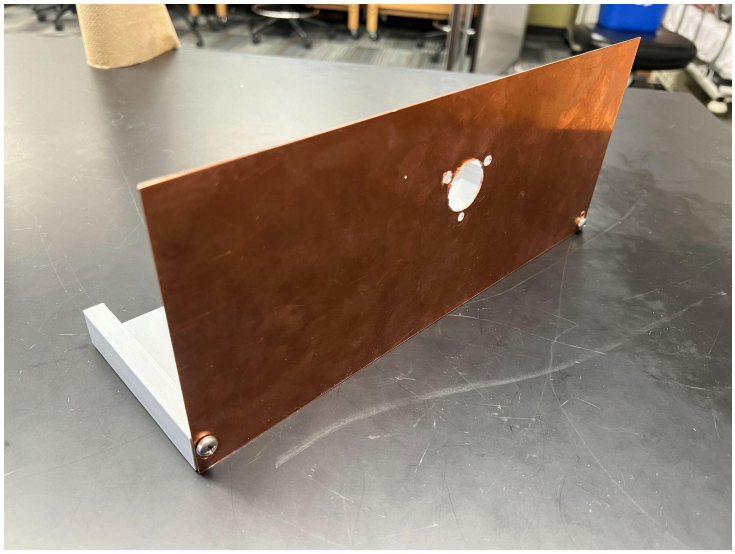

Figure 5: Motor stand and Face connected

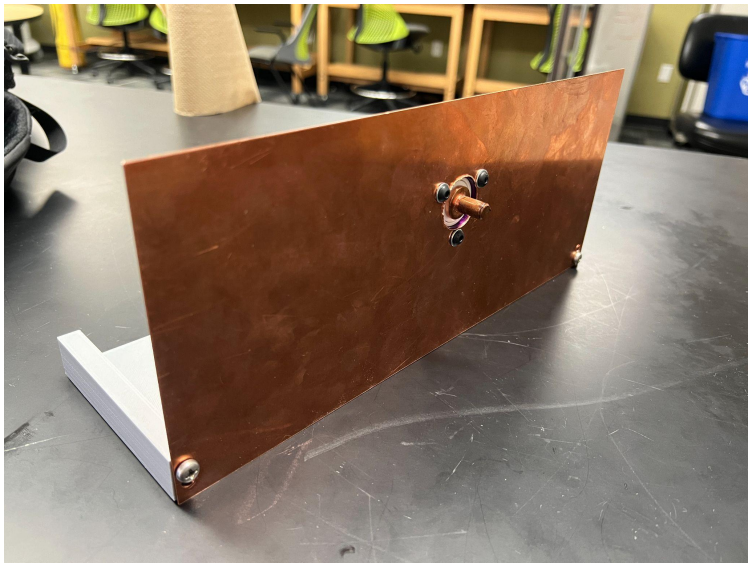

Figure 6: Motor connected to Motor stand

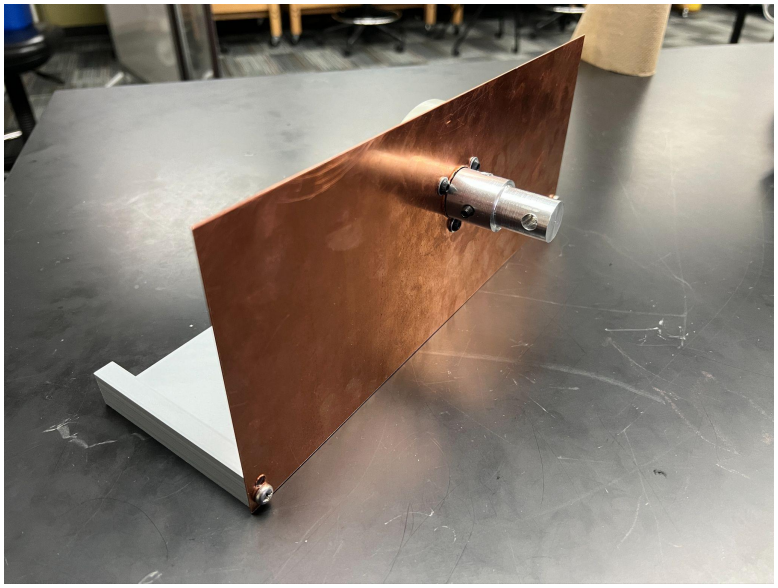

Figure 7: Motor to Driveshaft Adapter connected

1. Using two M5 screws, attach copper face to copper stand. One screw on each side staggered, as illustrated in figure 5.
2. Using three M4 and three M4 washers, connect the piezoelectric motor to the copper face. Motor cable connection should point down, as illustrated in figure 6.
3. Slide the Motor to Driveshaft Adapter over the motor stud. Using a M4 screw, screw down onto one of the two flat sides of the motor stud to secure the adapter to the motor, as illustrated in figure 7.

Gearbox Assembly

3D Print Components

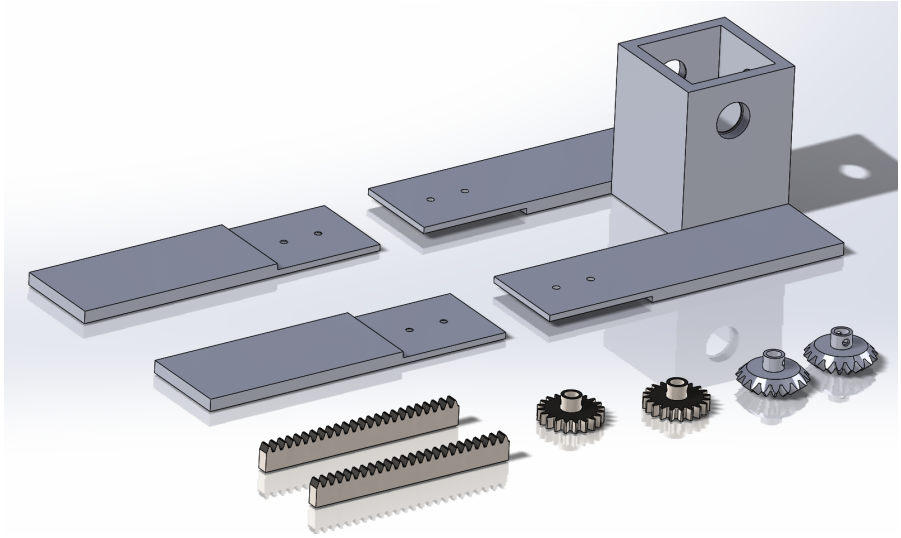

Figure 8: Gearbox 3D printed components

At the Makerspace, 3D print the Gearbox, Gearbox Extensions, Bevel Gears, Pinion Gears, and Rack Gears at 20% infill, as illustrated in figure 8.

Crosspin

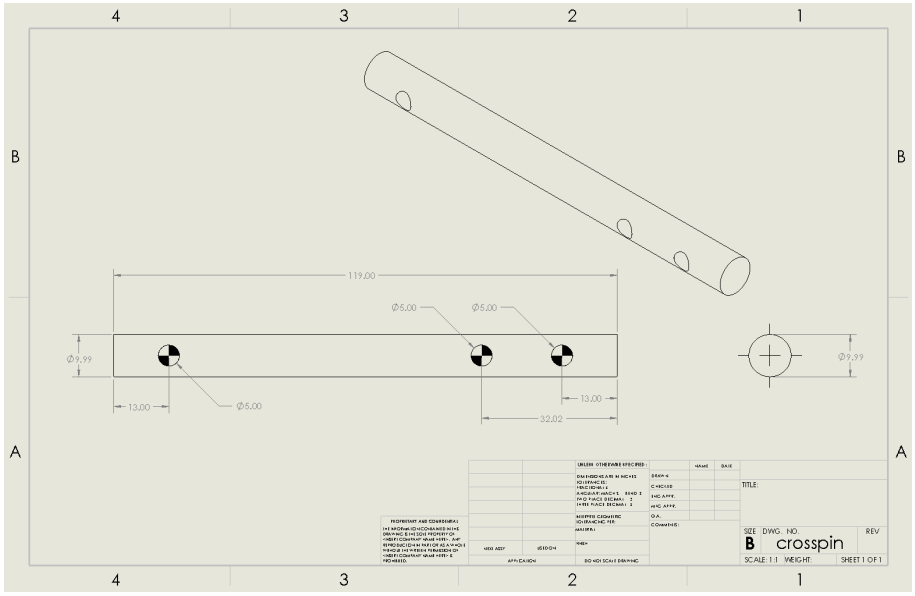

Figure 9: Crosspin drawing

1. In the TEAM Lab, start with 1” HDPE cylindrical stock. Lathe the piece down to 10mm diameter.
2. Using a 5mm bit, on the mill drill three holes in the crosspin in the locations illustrated in figure 9.

Gearbox to Driveshaft Adapter

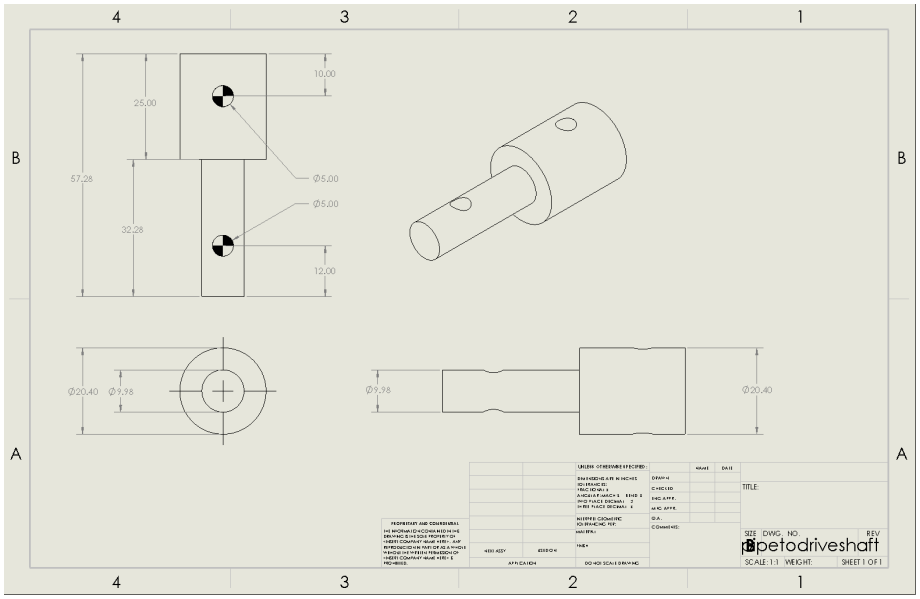

Figure 10: Gearbox to Driveshaft Adapter

1. In the TEAM Lab, start with 1” HDPE cylindrical stock. Lath 32.28mm length to 10mm diameter.
2. Lathe the next 25mm down to 20.4mm diameter.
3. Part the piece off to a 57.28mm length.
4. Using a 5mm bit, on the mill drill two holes in the adapter in the locations illustrated in figure 10.

Phantom Bed

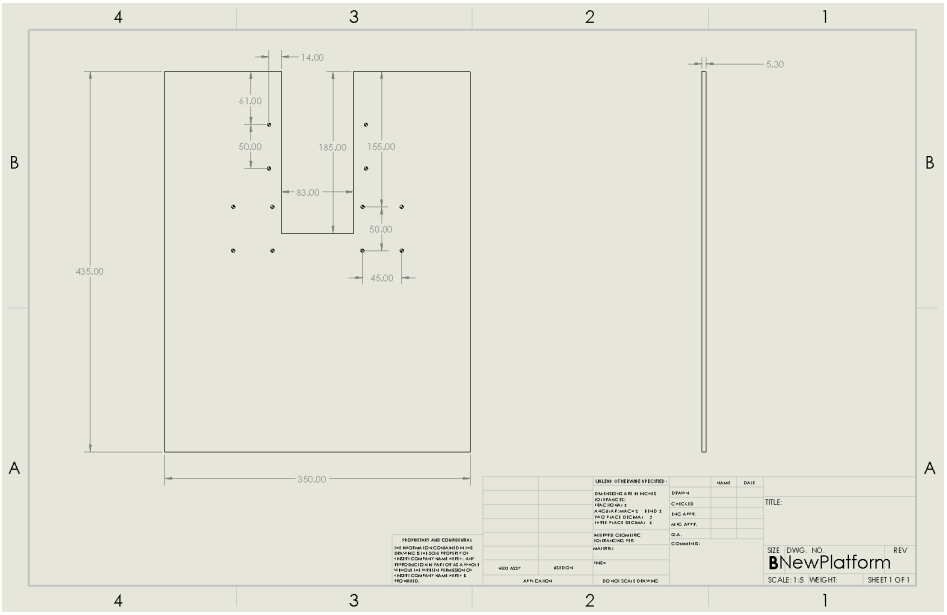

Figure 11: Phantom Bed drawing

1. In the TEAM Lab, cut an acrylic sheet to 350mm by 435mm on a table saw.
2. Using a bandsaw, cut a 83mm by 185mm rectangle from the center of the 350mm side, as illustrated in figure 11.
3. Using a drill press, drill 12 M4 holes according to the drawing illustrated in figure 11.

Full Gearbox Assembly

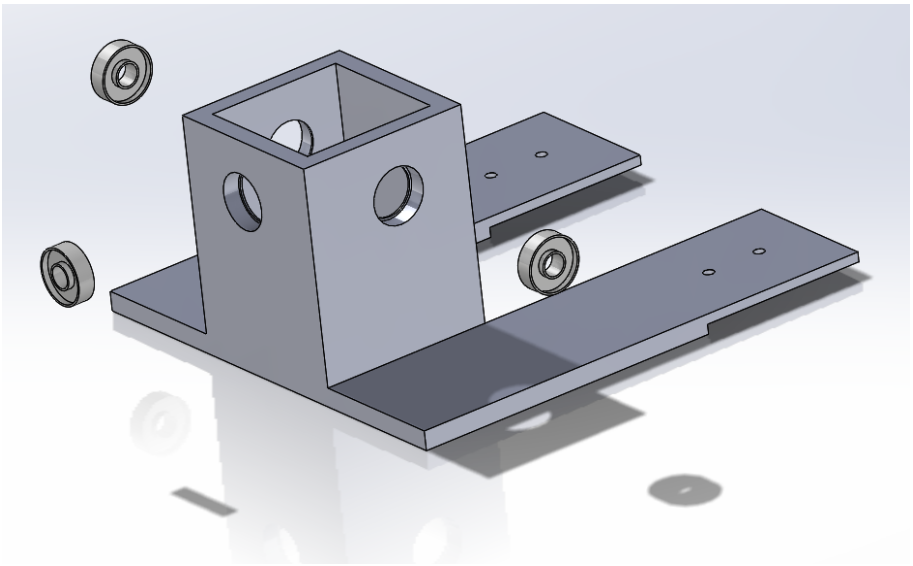

Figure 12: Adding bearings to gearbox

1. Insert three glass ball bearings into the gearbox as illustrated in figure 12.

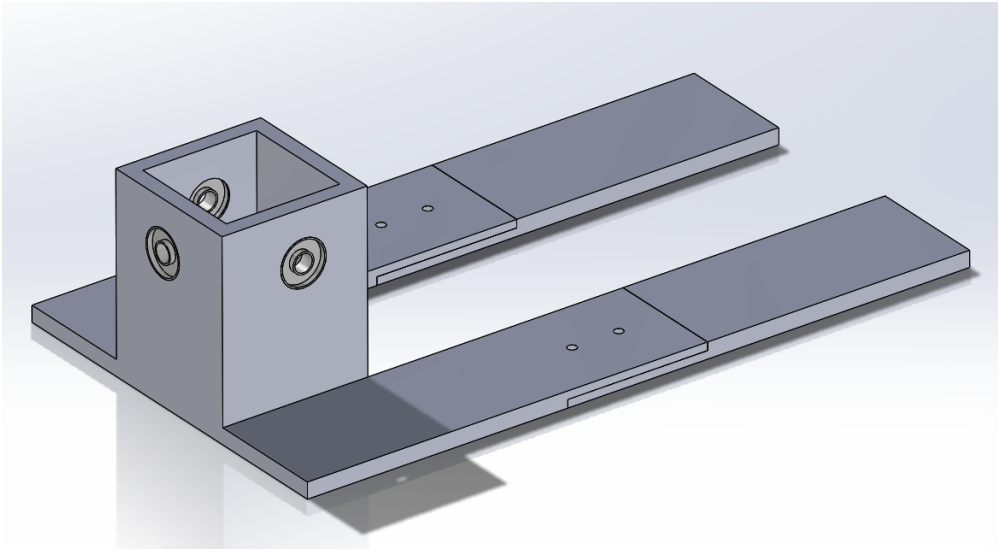

Figure 13: Adding Gearbox extensions

2. Connect 3D printed gearbox extension pieces to the gearbox via four M4 screws, as shown in figure 13. Screws should be screwed in from the bottom up.

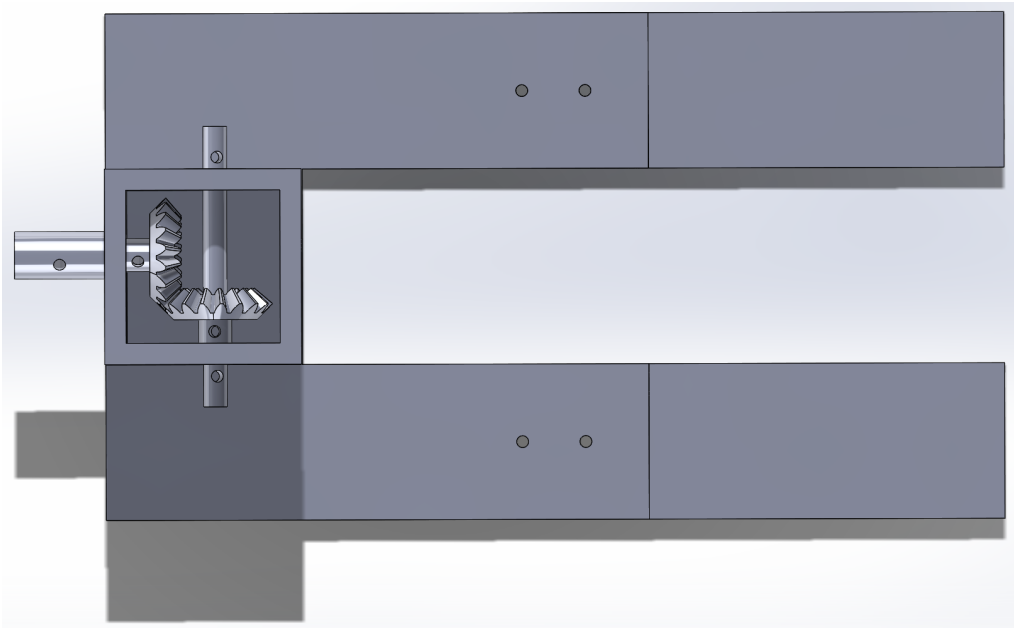

Figure 14: Adding internal components to gearbox

3. Add Gearbox to Driveshaft adapter, Crosspin, and bevel gears in the configuration illustrated in figure 14.
4. Using two M4 screws, anchor the bevel gears to the crosspin and adapter.

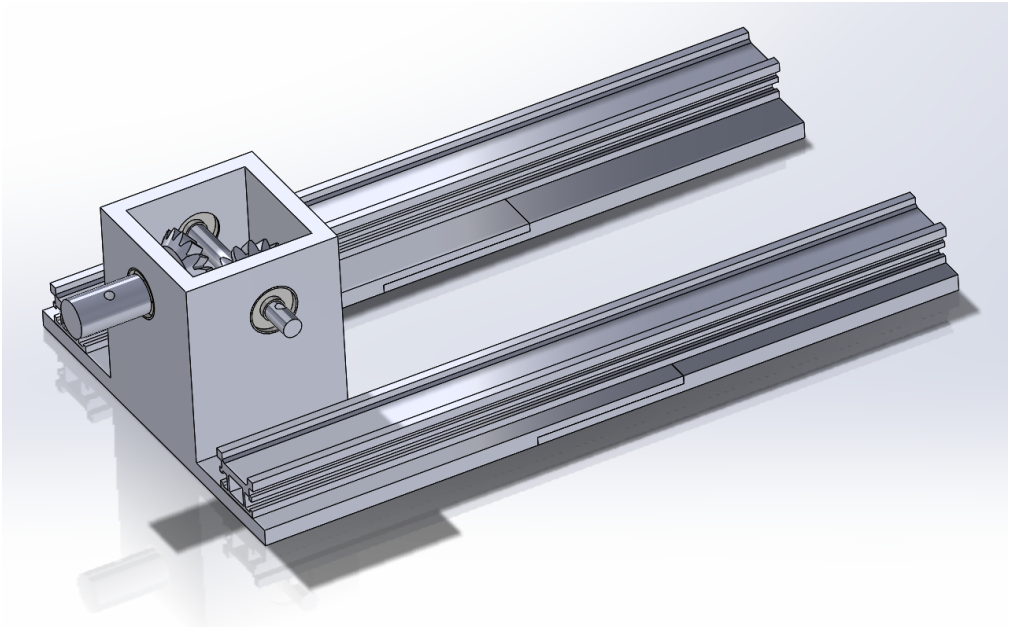

Figure 15: Adding linear rails to assembly

5. Using the same four M4 screws to connect the gearbox to the gearbox extensions, connect two linear rails as illustrated in figure 15.

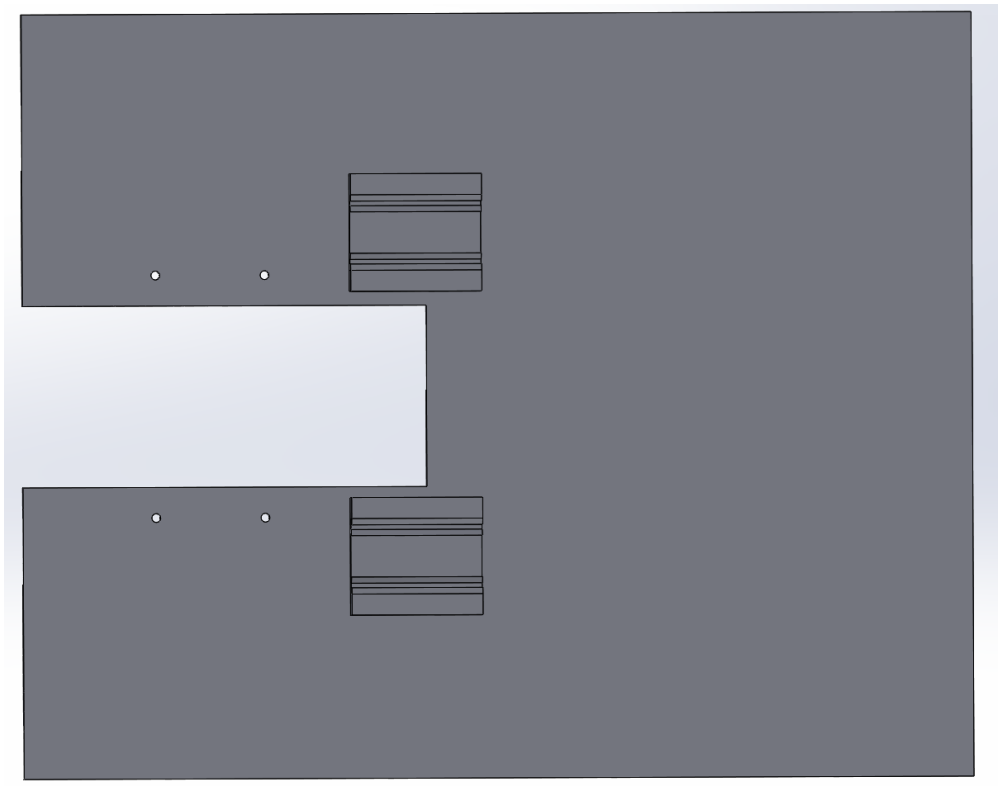

Figure 16: Adding linear slides to assembly

6. Using eight M4 screws, attach two linear slides to the bottom of the phantom bed as illustrated in figure 16.

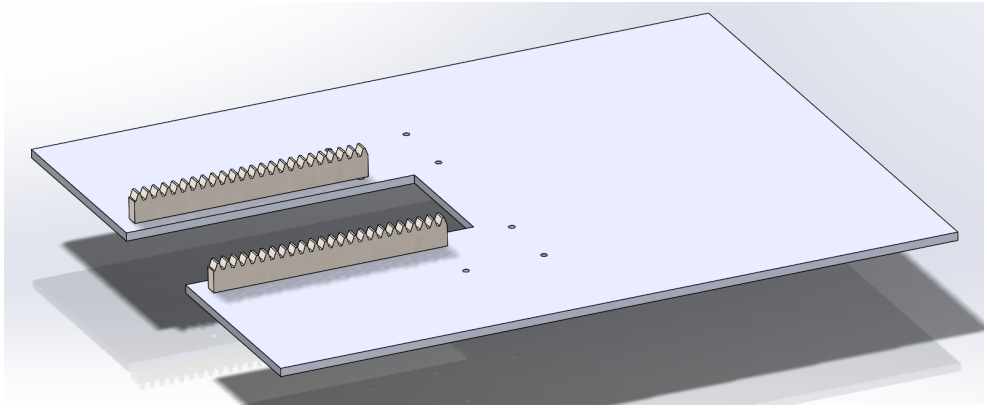

Figure 17: Adding rails to phantom bed

7. Using four M4 screws (two per rail) attach rails to the phantom bed as illustrated in figure 17.

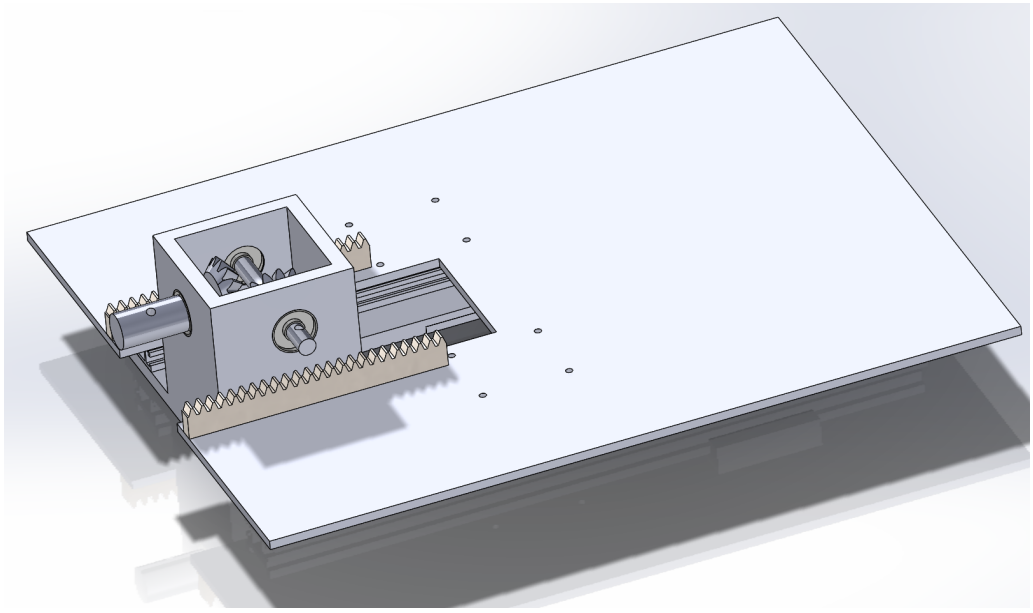

Figure 18: Adding phantom bed to gearbox

8. Slide the linear slides on the bottom of the phantom bed on top of the linear rails attached to the gearbox as illustrated in figure 18.

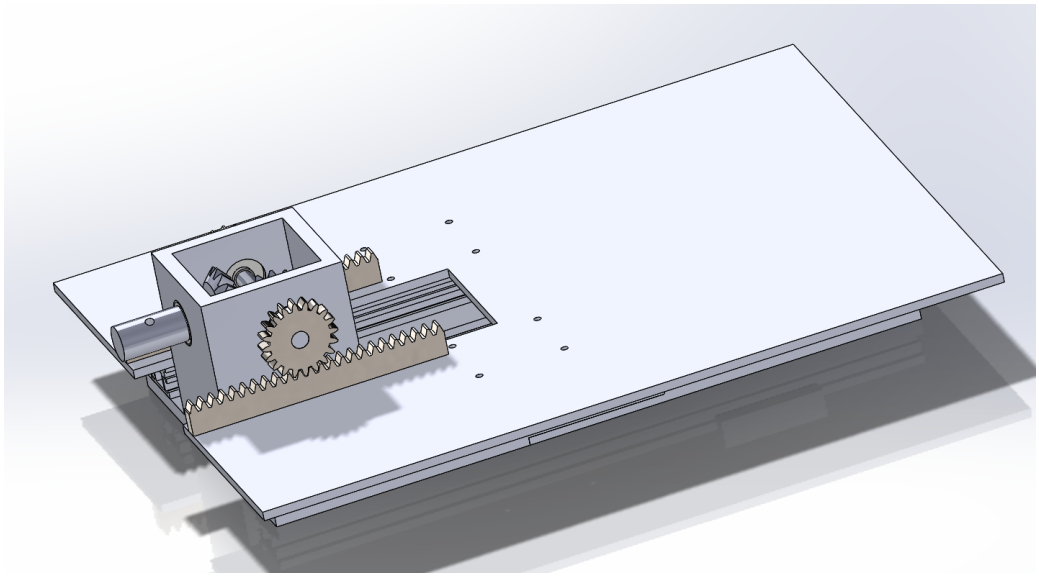

Figure 19: Adding pinion gears to assembly

9. Slide pinion gears onto both sides of the crosspin as shown in figure 19.
10. Using two M4 screws, anchor pinion gears to crosspin.

Driveshaft

1. Cut a 10’ long ¾” pvc pipe into half. Only one of the 5’ long pieces will be used in the full prototype assembly.

2. In the TEAM Lab, using a drill press, drill a 10mm hole 8mm from one end of the pipe.
3. Using a drill press, drill a 5mm 10mm from the other end of the pipe.

Full Prototype Assembly

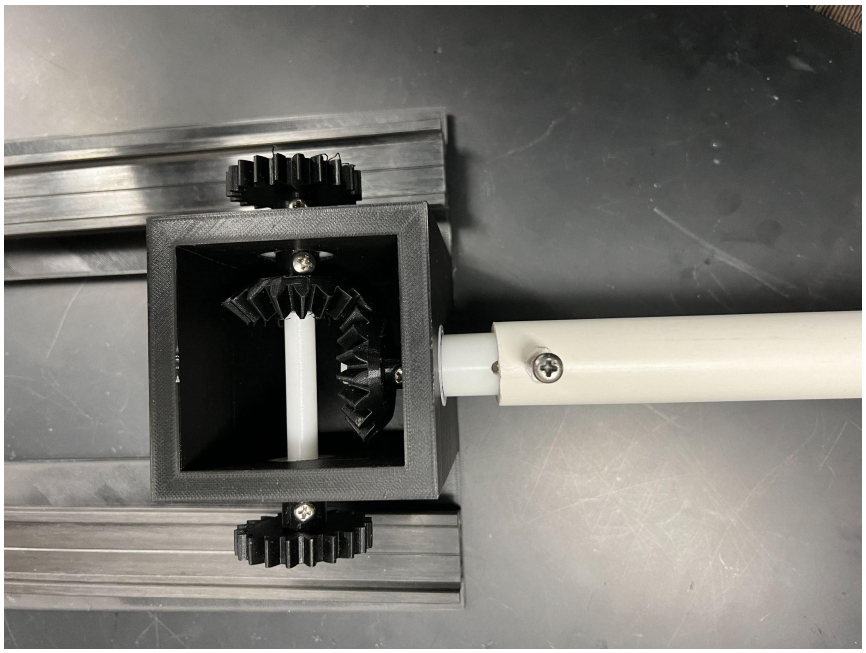

Figure 20: Attaching driveshaft to gearbox

1. Connect one side of the 5’ driveshaft to the gearbox to driveshaft adapter via a M5 screw.

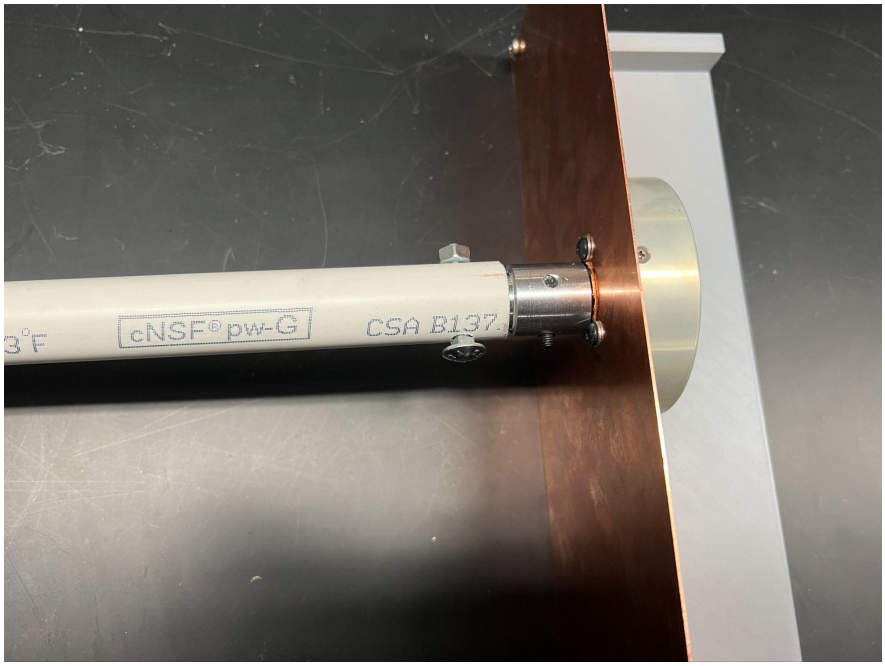

Figure 21: Attaching driveshaft to Motor assembly

2. Connect the other side of the 5’ driveshaft to motor assembly via a M10 screw and nut as illustrated in figure 21.


Figure 22: Full prototype assembly

3. Full prototype has been completed.

D. Testing Protocols
   a. Platform Sinusoidal Motion Test

Platform Sinusoidal Motion Test

Description:

This test is performed to determine if the platform is moving at the expected displacement of the sine wave. Multiple trials will be conducted at different weights. The motor velocity will be constant throughout trials.

Materials:

1. Fully assembled prototype
2. Bright marker
3. Camera
4. Kinovea software

Procedure:

1. Assemble complete prototype.
2. Connect the motor to the microcontroller and plug into power.
3. Connect the microcontroller to a laptop with the required files.
4. Ensure that the latest version of the active program is uploaded to the motor.
    a. The latest main.cpp can be downloaded from Lab Archives.
5. Place a bright marker on the platform to mark the initial position.
6. Set-up camera in full view of the platform and begin recording a video from the top view.
7. Run the function “sinusoidalSpeedVariation()” by pressing 2.
    a. This program will set the velocity of the motor to a sine wave with amplitude of 10 RPM, frequency of 8/60 Hz, and offset of 0. It will for 60 seconds
8. Once complete, stop recording the video.
9. Upload the video to Kinovea. Calibrate by drawing a line of known length on the video.
10. Place a tracking marker on the bright dot in the video. Track the displacement throughout the entire time the platform is moving.
11. Export the data to excel to perform statistical analysis.
12. Repeat steps 5-11 with different weights on the platform, ranging from 0-4 kg.

b. Motor RPM Test

Motor RPM Test

Description:

This test is performed to determine if the rotations per minute of the motor is accurate. At programmed speeds the prototype will be assessed to how accurate the physical speed is compared to the expected speed. At least 5 trials will be conducted for each set speed. The load will be constant throughout the trials.

Materials:

1. Ultrasonic Motor
2. Microcontroller & Wires
3. Post-It flag
4. Camera
5. Kinovea software

Procedure:

1. Connect the motor to the microcontroller and plug into power.
2. Connect the microcontroller to a laptop with the required files.
3. Ensure that the latest version of the active program is uploaded to the motor.
    a. The latest main.cpp can be downloaded from Lab Archives.
4. Place a thin post-it flag on the motor shaft to mark an initial position.
5. Set-up camera in full view of the platform and begin recording a video.
6. Run the function “motorRPMTest()” by pressing 5.
    a. This program will rotate the motor at 20 RPM until the encoder counts 1 revolution.
7. Once complete, stop recording the video.
8. Compare the time to complete the rotation to the expected time.
9. Repeat steps 4-8 until 5 or more trials are completed.
10. Repeat the procedure for a speed of 40 RPM and 60 RPM.

c. Motor Encoder Test

Motor Encoder Test

Description:

This test is performed to determine if the number of revolutions counted by the motor encoder is accurate.

Materials:

1. Ultrasonic Motor
2. Microcontroller & Wires
3. Post-It flag
4. Stopwatch

Procedure:

1. Connect the motor to the microcontroller and plug into power.
2. Connect the microcontroller to a laptop with the required files.
3. Ensure that the latest version of the active program is uploaded to the motor.
    a. The latest main.cpp can be downloaded from Lab Archives.
4. Place a thin post-it flag on the motor shaft to mark an initial position.
5. Run the function “revolutionsCounter()” by pressing 4 and start a stopwatch at the same time.
    a. This program will rotate the motor at 60 RPM until the encoder counts 60 revolutions.
    b. This program is expected to run for 60 seconds.
6. While the program is running, visually count the actual number of revolutions.
7. Compare actual number of revolutions against expected value. Make a note if the motor does not end in the same orientation as it started.
8. Repeat 3-5 times.

E. Results Raw Data

Raw data from the RPM test

Trial Number	Expected RPM	Start Time (s)	End Time (s)	Duration for 1 Revolution (sec)	Actual RPM
1	20	0.05	3.6	3.55	16.90
2	20	0.15	5.22	5.07	11.83
3	20	0.05	3.83	3.78	15.87
4	20	0.05	3.76	3.71	16.17
5	20	0.05	3.5	3.45	17.39
6	40	0.05	2.45	2.4	25.00
7	40	0.05	2.33	2.28	26.32
8	40	0.05	2.33	2.28	26.32
9	40	0.05	2.23	2.18	27.52
10	40	0.05	2.18	2.13	28.17

11	60	0.7	1.62	0.92	65.22
12	60	0.98	1.9	0.92	65.22
13	60	0.1	1.55	1.45	41.38
14	60	0.08	1.77	1.69	35.50
15	60	0.08	1.38	1.3	46.15

F. Final Motor Code

```
#include "mbed.h"

#include "QEI.h"

#include "math.h"

#include "ttmathbig.h"

#include <cstdio>

#include <math.h>

#include <time.h>       /* time_t, struct tm, difftime, time, mktime */

#include <stdlib.h>



BufferedSerial pc(USBTX, USBRX); //how to connect to terminal



// Setup for Encoder

QEI motorEncoder (D2, D3, D4, 5760,QEI::X4_ENCODING);

AnalogOut velocityControl(A2);

DigitalOut motorDirection(A0);

DigitalOut motorState(A1);



int motorIncrementsPerRev = 5400;
```

```
float hexaVelocity = 0.0;

float rpmVelocity;

float increment = 0;

float presicion = 0.015625;

float angle;

int demo;

int direction;

int state;

float  i = 0;

float sum;

float speed;



const float pi = 3.14159265;



// Define the maximum and minimum RPM values

const float maxRPM = 175.0; // Maximum RPM

const float minRPM = 5.0;   // Minimum RPM

const float slope = 3.3/(175); // max Volts / max RPM



// Define rack and pinion values

const float pinionDiameter = 43.45; // in mm
```

```
void returnToStart(){

    printf("Returning to Starting position");

    while (motorEncoder.getRevolutions() != 0) {

            velocityControl.write(0.15f);

            motorDirection.write(0);

            motorState.write(1);

        }

        motorState.write(0);

        printf("Motor in initial position \n\n");

        motorEncoder.reset(); //Sets the pulses and revolutions count to
zero.

}



// Function to vary the motor speed sinusoidally

void sinusoidalSpeedVariation() {

    printf("Sinusoidal Function \n\n");



    // printf("Enter desired Frequency \n\n");

    // char f;

    // pc.read(&f, 1);

    // int frequency = f - '0';



    // printf("Enter desired Amplitude \n\n");

    // char a;
```

```
    // pc.read(&a, 1);
    // int amplitude = a - '0';

    float amplitude = 10; //(maxRPM - minRPM) / 2.0;
    float offset = 0; //(maxRPM + minRPM) / 2.0;
    float frequency = 8.0/60; // Adjust the frequency as needed

    clock_t start = clock();

    bool condition = true;
    while(condition) {
        // Determine time since starting the loop
        clock_t end = clock();
        double currentTime = static_cast<double>(end - start) /
CLOCKS_PER_SEC;

        // Calculate the current RPM using a sinusoidal function
        float rpmVelocity = amplitude * sin(2 * pi * frequency *
currentTime) + offset;
        hexaVelocity = 0.0063 * rpmVelocity;

        if(hexaVelocity<0) {
            motorDirection.write(1); //CCW
            hexaVelocity = hexaVelocity*-1;
```

```
        } else {
            motorDirection.write(0); //CW
        }
        velocityControl.write(hexaVelocity);
        if(currentTime > 60.0) {
            condition = false;
        }
        motorState.write(1);
        //printf("End of loop \n");
    }
    printf("End of Function \n\n");
    returnToStart();
    motorState.write(0);
}


void incrementWrite()
{
    //printf("Enter a desired angle with a precision of 0.015625 degrees
\n");
    //scanf("%f", &angle);
    angle = 360; // hardcode angle
    increment = rint(angle / presicion);


    //scanf("%f", &rpmVelocity );
```

```
    rpmVelocity = 10; // hardcode rpmVelocity

    hexaVelocity = 0.0063*rpmVelocity;

    velocityControl.write(hexaVelocity);

    //printf("Enter 1 to start the motor rotation \n");

    //scanf("%d", &state);

    state = 1; //start motor rotation

    while (motorEncoder.getPulses() != increment) {

        if (motorEncoder.getPulses() < increment) {

            motorDirection.write(0); //clockwise

            motorState.write(1);

        }

        if (motorEncoder.getPulses() > increment) {

            motorDirection.write(1); //counter-clockwise

            motorState.write(1);

        }

        if (motorEncoder.getPulses() == increment) {

            motorState.write(0);

        }

    }

    motorState.write(0);

    printf(" Motor arrived at desired position \n\n");

}
```

```
void continuousMode()

{

    //printf("Enter a rotational speed between 5 and 175 rpm \n");

    //scanf("%f", &rpmVelocity);

    rpmVelocity = 10; // hardcoded

    hexaVelocity = 0.0063*rpmVelocity;

    velocityControl.write(hexaVelocity);

    //printf("Enter a rotational direction : 0 clockwise and 1
counterclockwise \n");

    //scanf("%d", &direction);

    direction = 0; //clockwise

    motorDirection.write(direction);

    //printf("Enter 1 to start the motor rotation \n");

    //scanf("%d", &state);

    state = 1;

    //printf("The motor will turn in the direction and the speed you chose
\n\n");

    int i = 0; // run for 10 seconds

    while ( state == 1) {

        motorState.write(state);

        //printf("Enter 0 to stop the motor \n\n");

        //scanf("%d", &state);

        wait_us(1000000); // wait 1 s

        if (i==10) {
```

```
            state = 0;

        }

        else{

            i = i+1;

        }

    }

    printf("%d",motorEncoder.getRevolutions());

    printf("%d",motorEncoder.getPulses());

    printf("\n\n");

    motorState.write(0);

    printf(" Motor stopped \n\n");

}



double distanceTraveled() {

    // calculate the distance traveled in mm

    // TODO: test accuracy, make more precise using pitch!

    double distance = motorEncoder.getPulses() * 3.14159265 *
pinionDiameter / motorIncrementsPerRev;

    return distance;

}



// rotate the motor at 60 RPM until encoder counts 60 revolutions

void revolutionsTest(){

    hexaVelocity = 60*.0063; // 60 RPM, (1.13275 is an experimental value)
```

```
    velocityControl.write(hexaVelocity);

    motorDirection.write(0); //CW

    increment = rint(360*60 / presicion);

    while(motorEncoder.getPulses()<increment){

        motorState.write(1);

        //printf("%d",motorEncoder.getRevolutions());

    }

    motorState.write(0);

    printf("%d",motorEncoder.getRevolutions());

    printf("Test is Completed \n\n");

}



//

void motorRPMTest(){

    hexaVelocity = 60*.0063; // RPM

    velocityControl.write(hexaVelocity);

    motorDirection.write(0); //CW

    increment = rint(360 / presicion);

    while(motorEncoder.getPulses()<increment){

        motorState.write(1);

    }

    motorState.write(0);

    printf("%d",motorEncoder.getRevolutions());
```

```
    printf("1 revolution counted. Test is Completed \n\n");

}




int main()

{

    //printf("Searching for initial position of the motor using the index
of the encoder \n\n");

    printf("Checking if initial position is at 0 \n\n");

    returnToStart();

    if(motorEncoder.getRevolutions() !=0) {

        printf("Motor is NOT in initial position. Calling Return to Start.
\n\n");

        returnToStart();

    }

    wait_us(500000*2);

    //incrementWrite(); // hardcoded version

    //continuousMode(); // hardcoded version

    //sinusoidalSpeedVariation();

    bool isOn = true;

    while(isOn) {

        printf("Enter 0 to Exit, Enter 1 for incrementWrite() hardcoded
demo, Enter 2 for sinusoidal demo, Enter 4 for revolutions test, Enter 5
for RPM test \n\n");

        char c;
```

```
        pc.read(&c, 1);
        int demo = c - '0';


        if ( demo == 1) {
            printf("Demo 1 Selected \n\n");
            incrementWrite();
            //continuousMode();
            motorEncoder.reset();
        }
        if ( demo == 2) {
            printf("Demo 2 Selected \n\n");
            sinusoidalSpeedVariation();
            motorEncoder.reset();
        }
        if( demo == 0) {
            printf("Exiting loop \n\n");
            isOn = false;
            motorState.write(0);
        }
        if ( demo == 4) {
            printf("Demo 4 Selected \n\n");
            //revolutionsInTime();
            revolutionsTest();
```

```
            motorEncoder.reset();

        }

        if ( demo == 5) {

            printf("Demo 5 Selected \n\n");

            //revolutionsInTime();

            motorRPMTest();

            motorEncoder.reset();

        }

    }

    printf("This is the end of the code \n\n");

}
```